Since January 2020 Elsevier has created a COVID-19 resource centre with free information in English and Mandarin on the novel coronavirus COVID-19. The COVID-19 resource centre is hosted on Elsevier Connect, the company's public news and information website.

Article

Immunity

COVID-19 immune signatures reveal stable antiviral T cell function despite declining humoral responses

Graphical Abstract

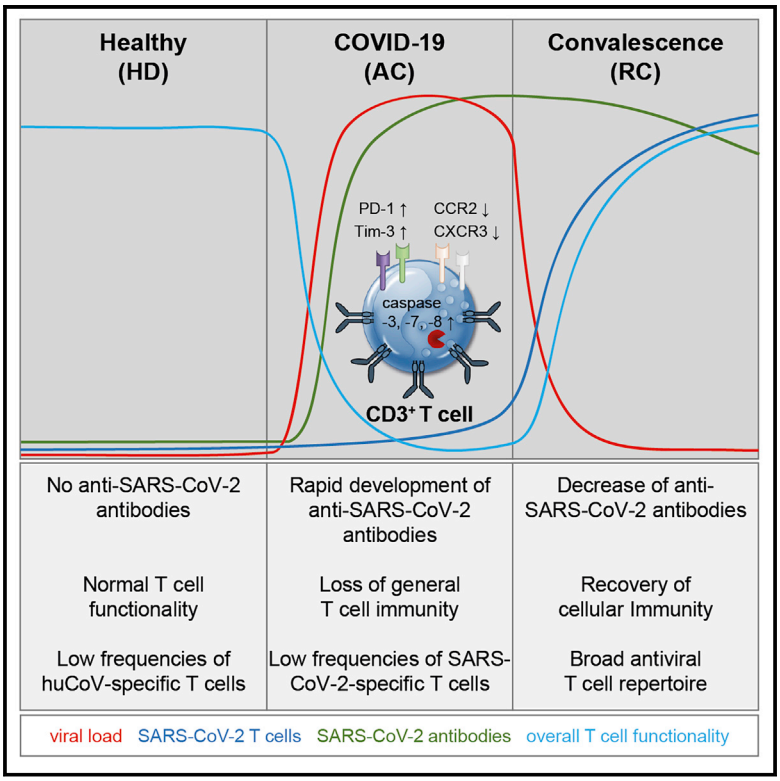

Highlights

- high SARS-CoV-2 IgG but overall reduced T cell immunity in active COVID-19 patients
- PD-1, Tim-3, and active caspases in T cells result in impaired T cell function
- stable SARS-CoV-2 T cell repertoire yet declining humoral responses during recovery
- potentially protective role of pre-existing anti-huCoV $CD4^+$ and $CD8^+$ T cell immunity

Authors

Agnes Bonifacius, Sabine Tischer-Zimmermann, Anna C. Dragon, ..., Oliver Witzke, Rainer Blasczyk, Britta Eiz-Vesper

Correspondence

eiz-vesper.britta@mh-hannover.de

In Brief

COVID-19 varies from asymptomatic infection to multiorgan failure, but data on cellular immunity against SARS-CoV-2 during disease and beyond are lacking. Bonifacius et al. show a beneficial effect of preexisting immunity to endemic coronaviruses during disease and stable cellular immunity with concomitant decrease of humoral responses early during convalescence.

Bonifacius et al., 2021, Immunity *54*, 340–354
February 9, 2021
https://doi.org/10.1016/j.immuni.2021.01.008

CellPress

CellPress

Immunity

Article

COVID-19 immune signatures reveal stable antiviral T cell function despite declining humoral responses

Agnes Bonifacius,[1] Sabine Tischer-Zimmermann,[1] Anna C. Dragon,[1] Daniel Gussarow,[1] Alexander Vogel,[1] Ulrike Krettek,[1] Nina Gödecke,[1] Mustafa Yilmaz,[2] Anke R.M. Kraft,[3,4,5] Marius M. Hoeper,[6] Isabell Pink,[6] Julius J. Schmidt,[7] Yang Li,[8] Tobias Welte,[6] Britta Maecker-Kolhoff,[9] Jörg Martens,[1] Marc Moritz Berger,[10] Corinna Lobenwein,[11] Metodi V. Stankov,[4,12] Markus Cornberg,[3,4,5] Sascha David,[7,13] Georg M.N. Behrens,[4,12] Oliver Witzke,[11] Rainer Blasczyk,[1,15] and Britta Eiz-Vesper[1,14,15,*]

[1]Institute of Transfusion Medicine and Transplant Engineering, Hannover Medical School, Hannover, Germany
[2]Public Health Department, Hannover, Germany
[3]Department of Gastroenterology, Hepatology and Endocrinology, Hannover Medical School, Hannover, Germany
[4]German Center for Infection Research (DZIF), partner site Hannover-Braunschweig, Germany
[5]Centre for Individualised Infection Medicine (CiiM), Hannover, Germany
[6]Department of Pneumology, Hannover Medical School, member of the German Centre for Lung Research (DZL), Hannover, Germany
[7]Department of Kidney and Hypertension Diseases, Hannover Medical School, Hannover, Germany
[8]Department Computational Biology for Individualised Medicine, Centre for Individualised Infection Medicine (CiiM), Helmholtz Centre for Infection Research, Hannover Medical School, Hannover, Germany
[9]Department of Pediatric Hematology and Oncology, Hannover Medical School, Hannover, Germany
[10]Department of Anesthesiology and Intensive Care Medicine, University Hospital Essen, Essen, Germany
[11]Department of Infectious Diseases, West German Centre of Infectious Diseases, University Hospital Essen, University Duisburg-Essen, Germany
[12]Department of Rheumatology and Clinical Immunology, Hannover Medical School, Hannover, Germany
[13]Institute of Intensive Care Medicine, University Hospital Zurich, Switzerland
[14]Lead Contact
[15]These authors contributed equally
*Correspondence: eiz-vesper.britta@mh-hannover.de
https://doi.org/10.1016/j.immuni.2021.01.008

SUMMARY

Cellular and humoral immunity to SARS-CoV-2 is critical to control primary infection and correlates with severity of disease. The role of SARS-CoV-2-specific T cell immunity, its relationship to antibodies, and pre-existing immunity against endemic coronaviruses (huCoV), which has been hypothesized to be protective, were investigated in 82 healthy donors (HDs), 204 recovered (RCs), and 92 active COVID-19 patients (ACs). ACs had high amounts of anti-SARS-CoV-2 nucleocapsid and spike IgG but lymphopenia and overall reduced antiviral T cell responses due to the inflammatory milieu, expression of inhibitory molecules (PD-1, Tim-3) as well as effector caspase-3, -7, and -8 activity in T cells. SARS-CoV-2-specific T cell immunity conferred by polyfunctional, mainly interferon-γ-secreting CD4$^+$ T cells remained stable throughout convalescence, whereas humoral responses declined. Immune responses toward huCoV in RCs with mild disease and strong cellular SARS-CoV-2 T cell reactivity imply a protective role of pre-existing immunity against huCoV.

INTRODUCTION

SARS-CoV-2 infection was declared a pandemic by the World Health Organization (WHO) on March 11, 2020. Clinical manifestations of the resulting COVID-19 disease range from asymptomatic infection to acute respiratory failure and death. Seven to ten days after initial symptoms, COVID-19 progresses in a minority of patients to a severe illness requiring hospitalization, intensive care treatment, and mechanical ventilation (Huang et al., 2020; Zhou et al., 2020). Most patients have a mild course of COVID-19. The reasons for this as well as the question of whether and how long acquired COVID-19 immunity might protect against re-challenge, as described in rhesus macaques (Chandrashekar et al., 2020), are still unknown. However, cases of reinfection have been reported (AlFehaidi et al., 2020; Iwasaki, 2021).

In this context, reliable high-level evidence regarding adaptive antiviral immunity, its correlation with humoral responses, the temporal course of disease, and the potentially protective role of immunity against endemic coronaviruses (huCoV) is still lacking. The earliest detectable antibody (Ab) responses occur 3 days after the onset of symptoms, but seroconversion occurs within 7–14 days in the majority of patients (Huang et al., 2020;

Krammer and Simon, 2020; Zhou et al., 2020). Abs against the nucleocapsid (N) and the spike (S) protein are commonly detected (Amanat et al., 2020; Ni et al., 2020; Sekine, 2020) and Abs against the immunogenic receptor-binding domain (RBD) of the S protein act as potently neutralizing Abs by binding to human angiotensin-converting enzyme 2 (Ju et al., 2020; Vabret et al., 2020; Zhou et al., 2020). It has been reported that COVID-19 is accompanied by changes in the immune cell compartment including increased numbers of Ab-producing plasmablasts, and this correlated with disease severity (Kuri-Cervantes et al., 2020; Mathew et al., 2020). One group found a correlation between neutralizing Ab titers and the number of antiviral T cells (Grifoni et al., 2020; Ni et al., 2020). SARS-CoV-2-specific $CD4^+$ and $CD8^+$ T cells recognizing peptides derived from N, S, and membrane (M) protein are generally detected in 70%–100% of active and recovered patients (Baruah and Bose, 2020; Grifoni et al., 2020; Huang et al., 2020; Leung et al., 2020; Ni et al., 2020; Peng et al., 2020a; Vabret et al., 2020; Weiskopf et al., 2020). Specific T cells are also detected in Ab-seronegative family members with asymptomatic or mild disease (Sekine, 2020) and in a small proportion of non-exposed individuals, indicating cross-reactivity in individuals infected with huCoV (Braun et al., 2020; Kissler et al., 2020; Weiskopf et al., 2020).

In this study, samples collected from 82 non-infected controls (healthy donors, HDs), 204 recovered COVID-19 patients (RCs), and 92 hospitalized, active COVID-19 patients (ACs) were analyzed at different time points. The study focused on key issues regarding the relationship, magnitude, and composition of humoral and cellular SARS-CoV-2 immunity as well as the question of whether Abs, functional, and phenotypic characteristics of antiviral T cells, plasma cytokines and chemokines, and pre-existing huCoV-specific T cells are associated with the outcome of COVID-19. ACs exhibited generally low T cell responses, which largely were not dependent on lymphopenia, but rather on the role of programmed cell death protein 1 (PD-1) and T cell immunoglobulin and mucin domain-3 (Tim-3) as well as caspase-mediated apoptosis in T cells. High IgG ratios of SARS-CoV-2 Abs were observed in ACs, suggesting an early role of the humoral immune response. The fact that RCs exhibited broad and strong T cell responses and HDs had pre-existing T cells against M and S protein yet no SARS-CoV-2 Abs suggests a potentially protective role of pre-existing T cell immunity. In follow-up samples from RCs, Ab levels decreased over time while T cell frequencies remained stable.

Our results suggest that T cell immunity is important for lasting protection against SARS-CoV-2. Monitoring of COVID-19 patients and SARS-CoV-2-naive donors and the resulting knowledge about antiviral T cell and other immune cell function in combination with the occurrence of specific Abs will lead to a better understanding of the pathology, protective mechanisms, disease outcome predictors, and the success of vaccination strategies.

RESULTS

SARS-CoV-2 IgG ratios correlate with disease severity and decrease over time

Three cohorts were investigated in this study: HDs (n = 82), RCs (n = 204), and ACs (n = 92). None of the subjects had a history of transplantation or malignant disease. 90 ACs were hospitalized for COVID-19 and 2 for COVID-19-unrelated reasons (WHO score 2). 27 ACs were treated with remdesivir, 3 with dexamethasone, and 17 with both. None of the subjects received convalescent plasma. The average cohort age was 44 (range 18–68) years for HDs, 43 (19–68) years for RCs, and 60 (21–92) years for ACs (Figure S1A). SARS-CoV-2 ELISA for detection of Abs against N and S1 in plasma revealed that three HDs had IgG ratios defined as intermediate or positive results for one of the tested Abs, but negative results for the other (Figure 1A). Assessing anti-SARS-CoV-2 Abs in HDs with low pre-test probability requires confirmation of positive results from single measurements by alternative serology tests or functional assays (Behrens et al., 2020). Additional western blot-based testing of these samples using SARS-CoV-2 recomLine was negative. Thus, these results were considered false positive. In the RC cohort, n = 151 (75.9%) and n = 169 (84.9%) subjects had detectable loads of Abs against N and S1, respectively (double-positive: n = 137 [68.8%]), while n = 10 (5.0%) did not. Overall, SARS-CoV-2 IgG ratios in ACs were slightly higher than in RCs and significantly higher than in HDs. S1- and N-specific SARS-CoV-2 Abs were detected in 62.0% and 72.8% of ACs, respectively. All ACs except one seroconverted for at least one of the tested Abs during weekly follow-up monitoring (time post positive PCR: mean 13 days; range 0–49 days) (Figure 1B). Significant correlations between anti-N and -S1 IgG ratios were observed in both RCs and ACs (Figure 1C).

According to the Ordinal Scale for Clinical Improvement (WHO, 2020), all HDs had a WHO score of 0 (uninfected), 2.0% of RCs had a WHO score of 1 (ambulatory, no limitation of activities), 94.4% of 2 (ambulatory, limitation of activities), 3.1% of 3 (hospitalized, mild disease, no oxygen therapy), and 0.5% of 6 (hospitalized, severe disease, intubation, and mechanical ventilation). 60.9% of ACs had a WHO score of 1–4 (ambulatory to hospitalized, mild disease), and 39.1% of 5–7 (hospitalized, severe disease) (Figure 1C). The WHO scores for all cohorts significantly correlated with anti-N and -S1 IgG ratios. Since most RCs had mild disease with heterogeneous symptoms for a mean duration of 12 days (range 1–73 days), we used an internal Disease Severity Score (DSS) to further classify their symptoms. The results were as follows: no symptoms (n = 4, 2.0%), flu-like symptoms (n = 159, 81.1%), diarrhea or nausea (n = 20, 10.2%), fever (n = 90, 45.9%), respiratory symptoms (n = 138, 70.4%), neurological symptoms (n = 88, 44.9%), hospitalization (n = 7, 3.6%), and ventilation (n = 1, 0.5%). DSS significantly correlated with IgG ratios (Figure 1D). No correlation between DSS and age or sex was found (Figure S1B). Symptom duration in RCs correlated with age in males but not females (Figure S1B). Within RCs, no correlation between time of convalescence and IgG ratios was found (Figure 1D). The majority of ACs presented with high IgG ratios early during disease, and these remained stable or even increased during active disease (Figure 1B). However, analysis of individual RCs revealed a significant decrease in anti-N and -S1 IgG ratios over time (Figure 1D).

In summary, RCs and ACs were heterogeneous with respect to disease severity and IgG ratios and a correlation between disease severity and anti-N and -S1 IgG ratio during active disease and early recovery was found. High IgG ratios developed throughout the course of active disease indicating a functional

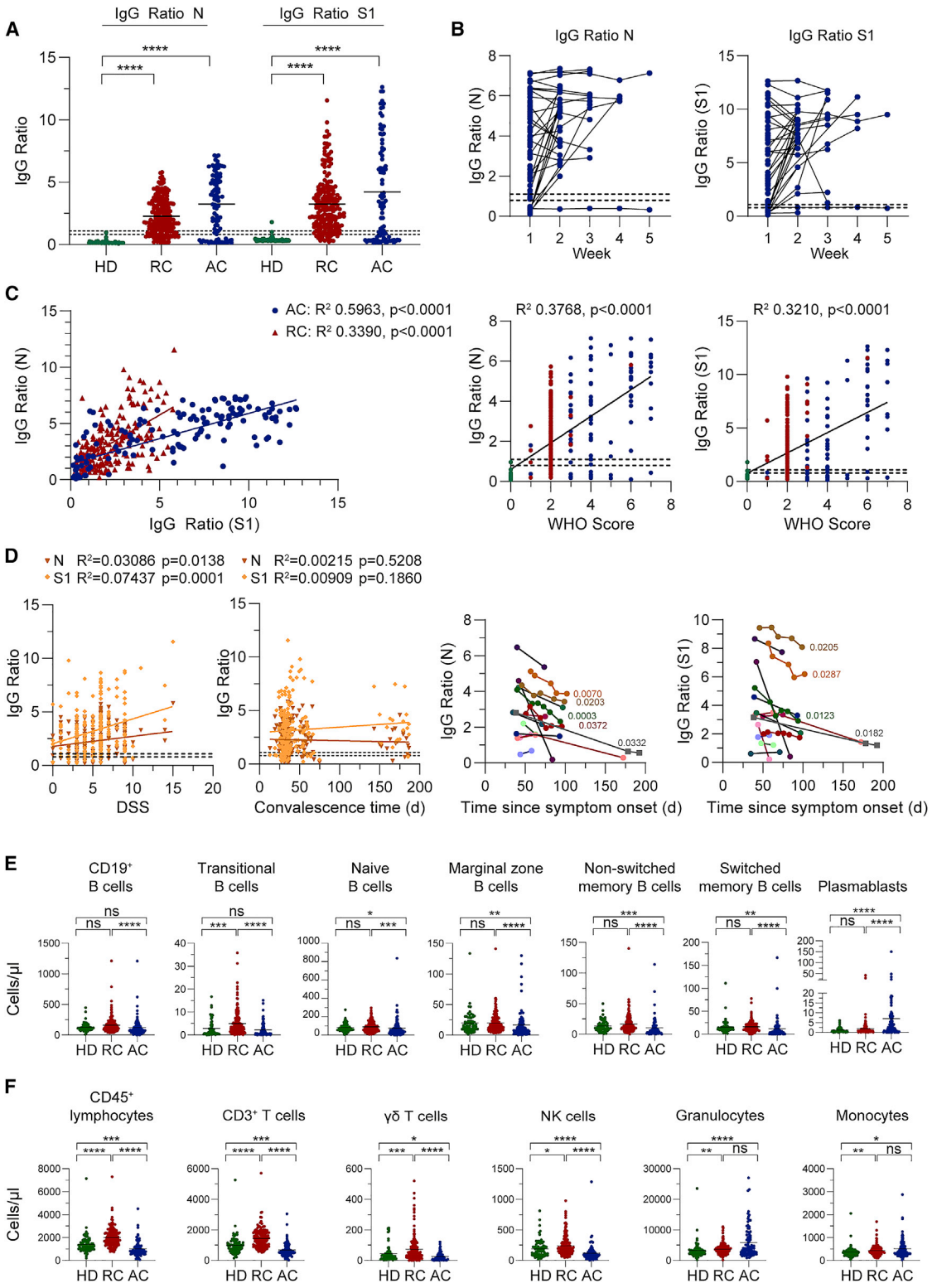

Figure 1. SARS-CoV-2 IgG ratios decline and COVID-19-associated humoral and cellular immune profile regresses throughout recovery

Shown are the SARS-CoV-2 humoral and cellular immune profiles of healthy donors (HD, green), recovered COVID-19 patients (RC, red), and patients with active COVID-19 (AC, blue).

(A) SARS-CoV-2 N and S1 IgG ratios in HDs, RCs, and ACs (first sample).

(legend continued on next page)

humoral immune response. Overall, it appears that Ab responses peak at around day 50 followed by a decline thereafter.

Cellular immune profile is altered during COVID-19 and regresses throughout recovery

The observed decrease in IgG ratios shortly after recovery suggested that humoral immune responses against SARS-CoV-2 alone did not provide long-term immunity. Immune phenotyping of whole blood samples was performed to characterize the cellular profile during and after SARS-CoV-2 infection (Figures 1E and 1F; Figures S1–S3). Compared to RCs and HDs, ACs had a distinct infection-associated B cell phenotype as indicated by significantly decreased numbers of total $CD19^+$ B cells along with decreased numbers of transitional ($IgD^+CD27^-CD38^{hi}$), naive ($CD27^-CD38^+CD24^-$), marginal zone (IgD^+CD27^+), non-switched ($IgD^+CD27^+CD38^{lo}$), and switched memory ($IgD^-CD27^+CD38^{lo}$) B cells (Figure 1E). ACs had significantly increased numbers of Ab-producing plasmablasts ($CD27^{hi}CD38^{hi}$) along with high anti-N and -S1 IgG ratios (Figure 1A). The regress of humoral immunity during convalescence was clearly indicated by a decrease of plasmablasts and an increase of transitional, naïve, and marginal zone B cells, coming closer to steady-state conditions found in the healthy population (Rudolf-Oliveira et al., 2015). The development of long-term humoral immunity elicited by SARS-CoV-2 infection was indicated by higher numbers of memory B cells in RCs when compared to ACs.

Consistent with previous reports (Huang and Pranata, 2020), ACs presented with overall reduction of lymphocyte and T cell counts (Figure 1F). All three cohorts had comparable $CD4^+$ and $CD8^+$ T cell ratios (Figure S1C), but RCs with intermediate DSS (3–7) had a slightly higher CD4/CD8 ratio than those with more severe disease (data not shown). In ACs, the T cell phenotype was characterized by decreased naive T cells (Tn) and a concomitant increase of $CD4^+$ central memory ($CD4^+$ Tcm) and $CD8^+$ effector memory T cells re-expressing CD45RA ($CD8^+$ Temra) (Figures S1C and S1D). The fraction of $CD4^+$ Tcm cells remained elevated during recovery (Figures S1D). ACs had reduced numbers of $\gamma\delta$ T cells and NK cells compared to HDs (Figure 1F). These cell subsets increased in RCs compared to HDs during convalescence. Compared to RCs and HDs, ACs had increased granulocyte and monocyte counts, which positively correlated with disease severity (Figure 1F; Figure S3A). Follow-up samples from individual RCs indicated that cellular immunity, determined mostly by the number of $CD45^+$ lymphocytes and granulocytes, regressed to a steady state (Figure S3B).

Overall, ACs exhibited the characteristic immunological cellular profile associated with the development of lymphopenia throughout the course of disease, distinguishing them from RCs and HDs. These results suggest a strong pro-inflammatory response during active disease and the restoration of cellular immunity during recovery.

Recovery from mild COVID-19 is associated with a broad anti-SARS-CoV-2 T cell repertoire

Frequencies of antiviral T cells against peptide pools derived from SARS-CoV-2, huCoV strains OC43 and 229E, Respiratory Syncytial Virus (RSV), Influenza A Virus (IAV), and Cytomegalovirus (CMV) were enumerated by interferon-gamma (IFN-γ)-enzyme-linked immunospot assay (ELISPOT). Each subject was classified as a non-responder (NR), low (LR), intermediate (IR), or high responder (HR) based on the results (Figure 2). 75.6% of HDs did not have SARS-CoV-2-specific T cells against any of the tested pools, whereas 15.5%, 11.9%, and 8.5% had M-, S-, and S2-specific T cells, respectively (Figure 2A). Most RCs had T cells against a broad variety of SARS-CoV-2-derived antigens (Figure 2B). 64.2%–72.1% exhibited T cells against M, N, S1, and S2, whereas only 45.6% had detectable T cells against S. Six of the ten RCs without SARS-CoV-2-specific Abs had specific T cells. In RCs, highest T cell frequencies were observed for M, S1, and S2; nevertheless, most RCs were classified as LR or IR. 85.9% of ACs exhibited SARS-CoV-2-specific T cells covering a broad spectrum of antigens throughout the course of disease (Figure S4A), but T cell frequencies were generally lower and very heterogeneous. Most responders were found for S1 (40%) and S2 (32%) (Figure 2C), and T cells against M, S1, and S2 were most frequent (mean number of spots per well [spw] 8.2, 10.2, and 11.0, respectively).

Overall T cell immunity, measured as the frequency of T cells specific for CMV phosphoprotein 65 (CMV_pp65) in CMV-seropositive subjects, was markedly lower in ACs than in RCs and HDs (mean spw: 34.2, 185.0, and 191.3, respectively). All CMV-seropositive RCs and HDs had detectable CMV_pp65-specific T cells, whereas 40 of 78 (51.3%) CMV-seropositive ACs did not. While RCs and HDs had comparable T cell frequencies specific for OC43_S and 229E_S, ACs had markedly lower frequencies against these antigens and against those from RSV and IAV. RCs had lower frequencies of RSV- and IAV-specific T cells than HDs even though they had recovered from lymphopenia. Moreover, RCs with no detectable SARS-CoV-2-specific T cells also had lower fractions of responders

(B) Seroconversion during COVID-19, expressed as anti-N and -S1 IgG ratios during weekly follow-up of ACs. Dashed lines indicate cutoff values for negative (< 0.8) and intermediate IgG ratios (0.8–1.1).
(C) Left: Correlation between anti-N and -S1 IgG ratios in RCs and ACs (first sample). Right: Association between WHO score and SARS-CoV-2 antibodies. Dashed lines indicate cutoff values for negative and intermediate IgG ratios.
(D) Left: Correlation between disease severity score (DSS) or time of convalescence and SARS-CoV-2 IgG ratios. Right: SARS-CoV-2 IgG ratios over time in individual RCs. Each symbol and color represent data from one RC; numbers behind the lines indicate p values for the corresponding individual.
(E and F) Cellular profile was determined by flow cytometric analysis of whole blood.
(A–C) n = 76–82 (HD), n = 199–204 (RC), and n = 92 (AC; first sample).
(D) Left: n = 199; right: n = 16.
(E–F) n = 63–79 (HD), n = 171 (RC), and n = 91–92 (AC).
(A, E, and F) Kruskal-Wallis test and Dunn's test for multiple comparisons or (C and D) linear regression analysis was used to calculate statistical significance: *p < 0.05, **p < 0.01, ***p < 0.001, ****p < 0.0001.
See also Figures S1–S3.

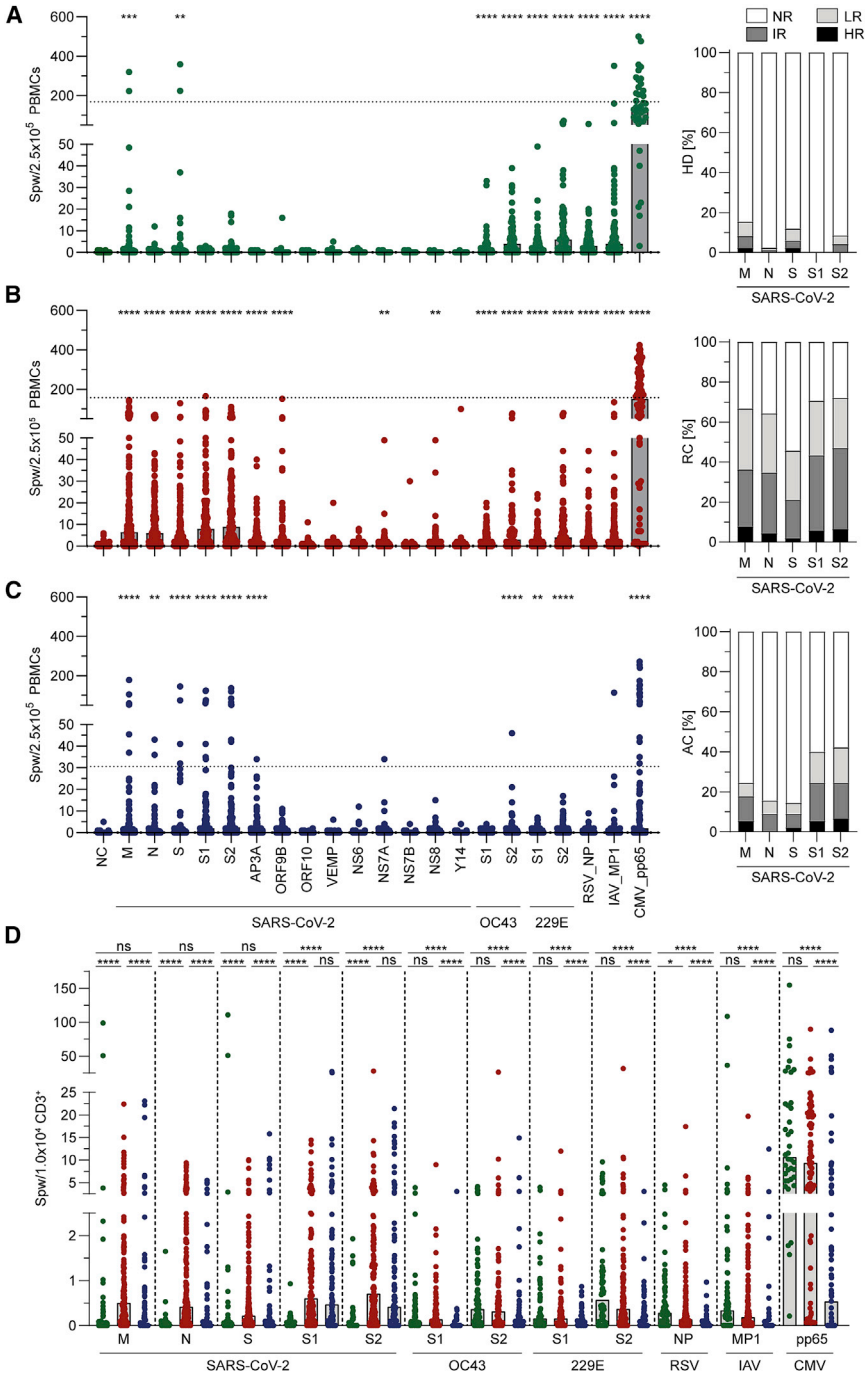

Figure 2. Recovery from mild COVID-19 is associated with a broad anti-SARS-CoV-2 T cell repertoire

(A–C) IFN-γ ELISPOT data from (A) healthy donors (HD, green, n = 48–82), (B) recovered COVID-19 patients (RC, red, n = 110–204), and (C) patients with active COVID-19 (AC, blue, n = 86–92; first sample) are depicted as the number of spots per well (spw)/2.5x10^5 PBMCs on the left side. For CMV_pp65 only values for seropositive individuals are depicted. The corresponding frequencies of non- (NR), low (LR), intermediate (IR), and high responders (HR) are shown on the right side.

(D) Inter-cohort comparison of antiviral T cell frequencies determined by ELISPOT assay normalized to T cell frequencies within PBMCs, depicted as spw/1.0x10^4 CD3$^+$ T cells. Statistical significance was calculated by Kruskal-Wallis test and Dunn's test for multiple comparisons.

(A–C) Statistically significant differences to negative control (NC) are depicted. *p < 0.05, **p < 0.01, ***p < 0.001, ****p < 0.0001.

See also Figure S4.

for RSV and IAV (data not shown), indicating an overall reduction of T cell immunity in these subjects.

To adjust for differences due to the observed reduction of T cell frequencies in ACs, ELISPOT data were normalized to the number of CD3$^+$ T cells within peripheral blood mononuclear cells (PBMCs) (Figure 2D; Figure S4B). The comparison showed that the differences in antiviral T cell frequencies observed in the three cohorts were independent of CD3$^+$ T cell numbers.

In summary, SARS-CoV-2-specific T cells were detected in all three cohorts. Post-recovery T cell responses were heterogeneous, and RCs exhibited the highest frequencies of antiviral T cells for M-, N-, and S-derived peptide pools. Both RCs and ACs had reduced RSV- and IAV-specific T cell frequencies compared to controls. In general, ACs had a reduced antiviral T cell repertoire, which did not seem to be caused by a reduction of T cell numbers alone.

Antiviral T cell repertoire remains stable during recovery from mild COVID-19

The finding that SARS-CoV-2 IgG ratios and infection-associated B cell subsets decreased during recovery from COVID-19 suggests an important role of T cell immunity (Figures 1D and 1E; Figure S3B). Analysis of the RC cohort showed that increasing DSS scores were generally associated with increasing M- and S-specific T cell frequencies but, paradoxically, subjects with a DSS > 6 had lower SARS-CoV-2-specific T cell frequencies (Figure 3A). Frequencies of T cells against M-, N-, and S-derived peptide pools not only remained stable but even became higher over the course of the convalescence period (Figure 3B). Analysis of follow-up samples from individual RC subjects collected up to 102 days after symptom onset revealed that T cell frequencies for SARS-CoV-2, huCoV, RSV, and IAV remained mostly stable (Figure 3C) and suggest the development of potentially protective T cell immunity during moderate COVID-19.

Together with the finding that active COVID-19 is associated with high SARS-CoV-2 IgG ratios but overall low T cell functionality, these results indicate that humoral immune responses

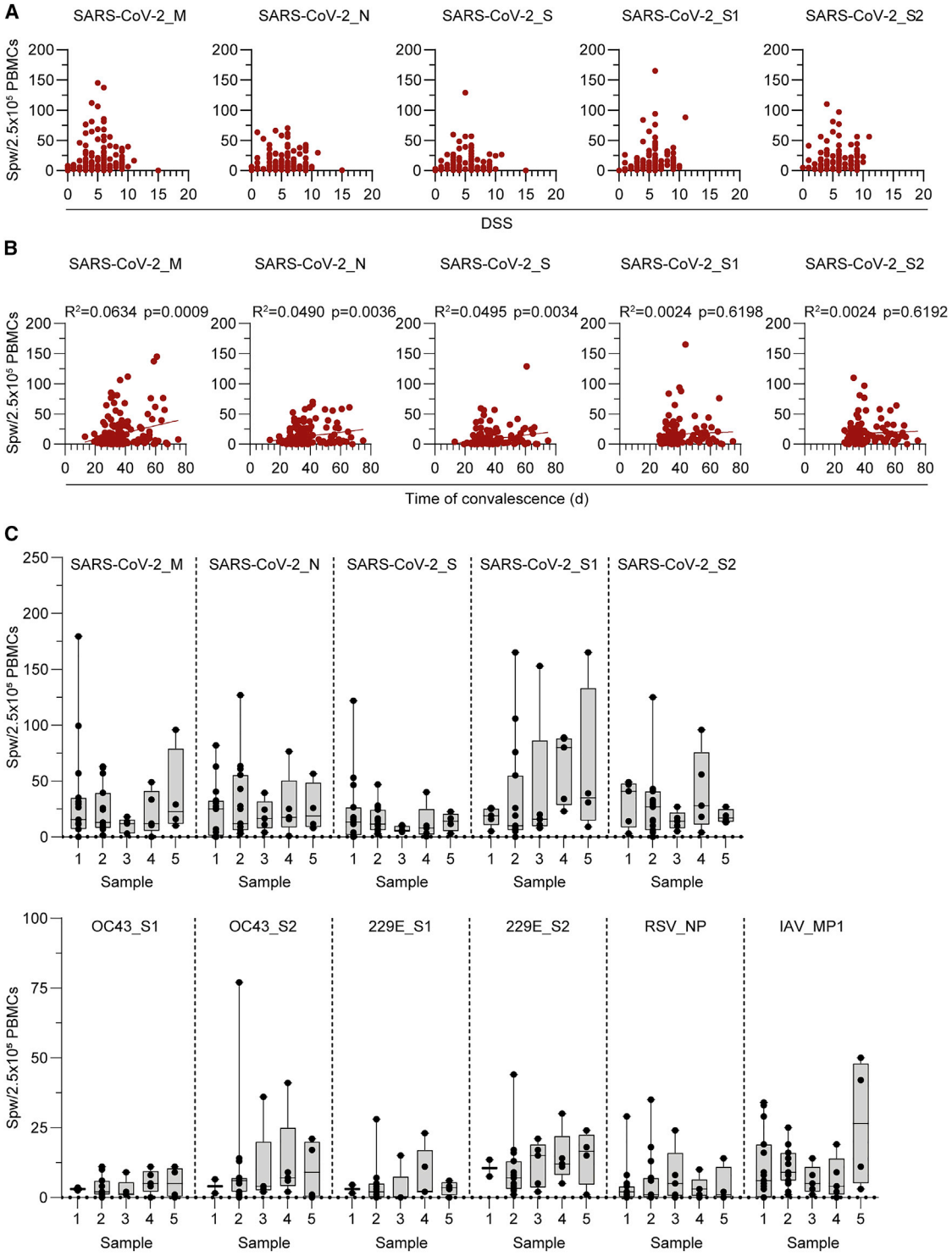

Figure 3. Antiviral T cell repertoire remains stable during recovery from mild COVID-19

(A) Antiviral T cell frequencies in relation to disease severity in recovered COVID-19 patients (RCs; red, n = 136–204).

(B) SARS-CoV-2_M-, N-, S-, S1-, and S2-specific T cell frequencies during convalescence in RCs (n = 110–178). Statistical significance was calculated by linear regression analysis.

(C) Frequencies of T cells specific for SARS-CoV-2 (upper panel), OC43, 229E, respiratory syncytial virus (RSV) and influenza A virus (IAV) (lower panel) in follow-up samples from RCs (n = 4–15).

See also Figure S4.

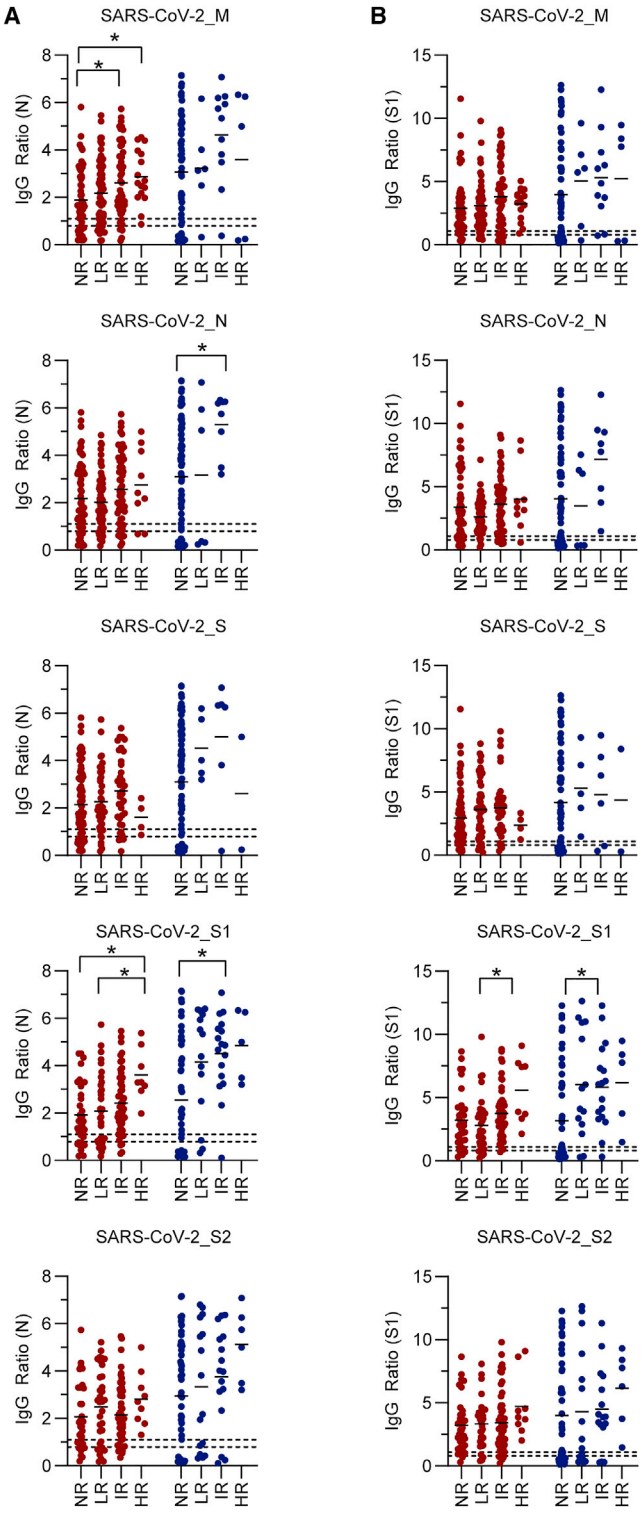

Figure 4. SARS-CoV-2 T cell frequencies partially correlate with SARS-CoV-2 IgG ratios

Recovered (RC, red, n = 131–199) and active COVID-19 patients (AC, blue, n = 90; first sample) were classified as non- (NR), low (LR), intermediate (IR), and high responders (HR) for the indicated antigens based on ELISPOT results. Dashed lines indicate cutoff values for negative and intermediate IgG ratios.

(A and B) Association between SARS-CoV-2-specific T cells and (A) anti-N or (B) anti-S1 IgG ratios. Statistical significance was calculated by Kruskal-Wallis test and Dunn's test for multiple comparisons. *p < 0.05.

plays an early role, whereas resolved mild COVID-19 appears to be associated with stable T cell immunity rather than long-lasting humoral immunity.

SARS-CoV-2 T cell frequencies partially correlate with SARS-CoV-2 IgG ratios

The diverse range of SARS-CoV-2 IgG ratios and T cell repertoires partly correlated with disease severity. To gain insight into whether there is an association between the establishment of humoral and cellular immunity against SARS-CoV-2, we investigated the relationship between SARS-CoV-2 IgG ratios and SARS-CoV-2-specific T cells in RCs and ACs. The results, shown as IgG ratios in the T cell responder groups, suggest that IgG ratios increased with increasing antiviral T cells (Figure 4). In the RC cohort, HR (mean IgG ratio 2.88) and IR (ratio 2.62) for SARS-CoV-2_M had significantly higher SARS-CoV-2_N IgG ratios than NR (ratio 1.90; Figure 4A). Within the AC cohort, SARS-CoV-2_N IR had significantly higher anti-N IgG ratios (ratio 5.31) than NR (ratio 3.10). Similar tendencies were found for M- and S-specific T cells. In the case of S1-specific T cells, both RCs and ACs with intermediate or high frequencies of antiviral T cells had higher amounts of Abs against N (RCs HR ratio 3.62, ACs IR ratio 4.52) and S1 protein (RCs HR 5.59, ACs IR 5.83) than NR or LR (N: RCs NR 1.93, RCs LR 2.09, ACs NR 2.55; S1: RCs LR 2.78, ACs NR 3.17; Figures 4A and 4B).

Overall, higher frequencies of SARS-CoV-2-specific T cells were found with higher SARS-CoV-2 IgG ratios, indicating some connection between humoral and cellular immunity in moderate cases of COVID-19.

COVID-19 patients with pre-existing T cell immunity against endemic coronaviruses have higher SARS-CoV-2_S-specific T cell frequencies

To study whether pre-existing T cell immunity against endemic huCoV strains OC43 and 229E was connected to SARS-CoV-2 T cell immunity, we correlated T cell frequencies for S-derived peptide pools S1 and S2 of SARS-CoV-2 with those for huCoV strains OC43 and 229E (Figure 5). As mentioned, HDs were heterogeneous with respect to OC43- and 229E-specific T cell frequencies, and some had high frequencies of SARS-CoV-2-specific T cells (Figure 2B). Although no significant correlation between frequencies of antiviral T cells against OC43 and 229E with SARS-CoV-2_S1- or S2-specific T cells was observed (Figures 5A and 5B), this did not exclude the possible presence of cross-reactive T cells. In RCs and in some ACs, subjects with higher OC43 or 229E_S-specific T cell frequencies exhibited higher numbers of SARS-CoV-2_S1 and SARS_CoV-2_S2-specific T cells. When testing plasma from 23 HDs, 20 RCs, and 10 ACs for the presence of huCoV-specific Abs, 61%, 45%, and 60% had OC43_N- and 87%, 75%, and 80% had 229E_N-specific Abs, respectively (Figure 5C). Some of those RCs lacked detectable huCoV-specific Abs but had huCoV-specific T cells. The latter finding is in line with reports showing waning huCoV-specific Abs over time but rapid functional immune responses upon second infection (Sariol and Perlman, 2020).

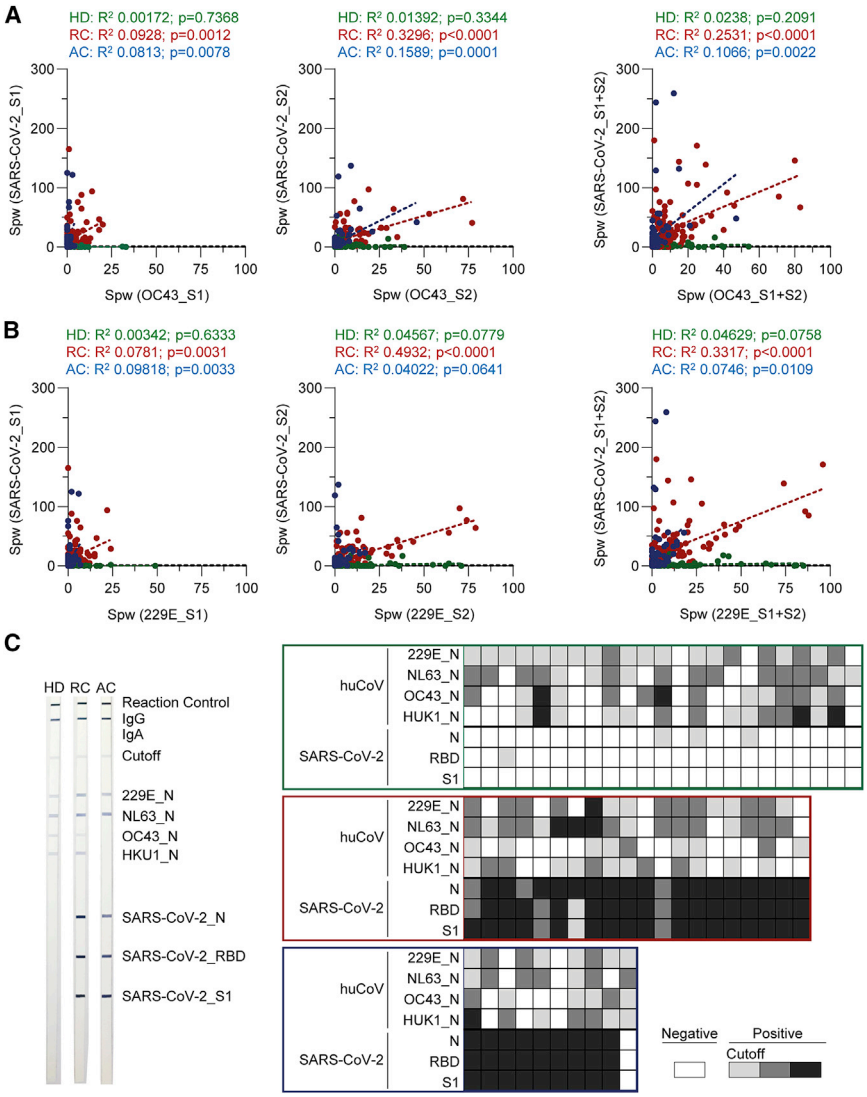

Figure 5. COVID-19 patients with pre-existing T cell immunity against endemic coronaviruses have higher SARS-CoV-2_S-specific T cell frequencies

(A) Correlation between OC43_S- and SARS-CoV-2_S-specific T cells in healthy donors (HD, green, n = 69), recovered (RC, red, n = 136) and active COVID-19 patients (AC, blue, n = 92; first sample).

(B) Correlation between 229E_S- and SARS-CoV-2_S-specific T cells in HDs (green, n = 69), RCs (red, n = 136) and ACs (blue, n = 92; first sample).

(A and B) Star-shaped symbols indicate RCs tested for huCoV-specific antibodies. Statistical significance was calculated by linear regression analysis.

(C) Exemplary western blots for SARS-CoV-2 and huCoV and summarized results from selected HDs (green), RCs (red) and ACs (blue, first sample). Each column represents data from one subject; the legend indicates signal strength.

Although ACs were heterogeneous with respect to SARS-CoV-2 T cells and their T cell responses against the common cold viruses were generally reduced, their SARS-CoV-2_S-specific T cells significantly correlated with OC43- and 229E-specific T cell frequencies, hinting toward cross-reactivity.

In summary, ACs and RCs with T cell immunity against huCoV strains OC43 and 229E exhibited higher SARS-CoV-2_S-specific T cell numbers. These results suggest that pre-existing cellular immunity against endemic huCoV might be beneficial for the development of SARS-CoV-2 T cell immunity and for disease outcome.

Overall impairment of T cell function contributes to reduced antiviral T cell immunity during COVID-19

There is evidence that a subset of COVID-19 cases is characterized by the development of a cytokine storm (Huang et al., 2020) as well as lymphopenia (Huang and Pranata, 2020). To gain insight into the underlying mechanism, cytokine and chemokine concentrations in plasma and expression of the respective receptor molecules were analyzed. As reported before for acute respiratory infection (Schögler et al., 2016), plasma IFN-γ-induced protein (IP-10) concentrations were significantly increased in ACs (mean 528.2 pg/mL) compared to HDs (mean 116.1 pg/mL) and RCs (mean 113.4 pg/mL) (Figure 6A). Frequencies of T cells expressing the corresponding cellular receptor, CXCR3, were significantly lower in ACs (mean 29.91%) than in HDs (mean 45.10%) and RCs (mean 48.87%). Moreover, ACs had significantly increased amounts of T cell polarization-associated cytokines IL-6 and IL-12p70, a sign of enhanced IP-10-induced T cell polarization (Figure 6B). While the frequencies of $CXCR3^+$ T cells and IP-10 concentrations in plasma were independent of disease severity, IL-6 concentrations in ACs were positively correlated with disease severity (Figures S5A and S5B). Plasma IL-2 concentrations in ACs were slightly lower than those in HDs and RCs, and those in RCs were higher than those in HDs (Figure 6B). In addition to CXCR3, independently of disease severity, frequencies of T cells expressing CCR2 were significantly reduced in ACs (mean 16.33%) compared to HDs (mean 27.92%) and RCs (mean 29.82%), whereas concentrations of its ligand, CCL2 (MCP-1), were highest in RCs, followed by ACs and HDs (Figure 6C; Figure S5C). Significantly higher amounts of soluble CD25 (sCD25) were detected in ACs compared to HDs and RCs but did not correlate with T cell counts in blood (Figure 6D; Figure S5D). ACs had high numbers of plasmablasts in conjunction with increased levels of sCD27, and this positively correlated with disease severity.

The reduced antiviral T cell functionality observed by ELISPOT is not necessarily caused by reduced T cell numbers but rather influenced by inhibitory molecules and immune checkpoint receptors. ACs had elevated frequencies of T cells expressing PD-1 (mean 28.79%) compared to HDs (mean 24.49%) and RCs (mean 21.31%), whereas soluble PD-1 concentration was

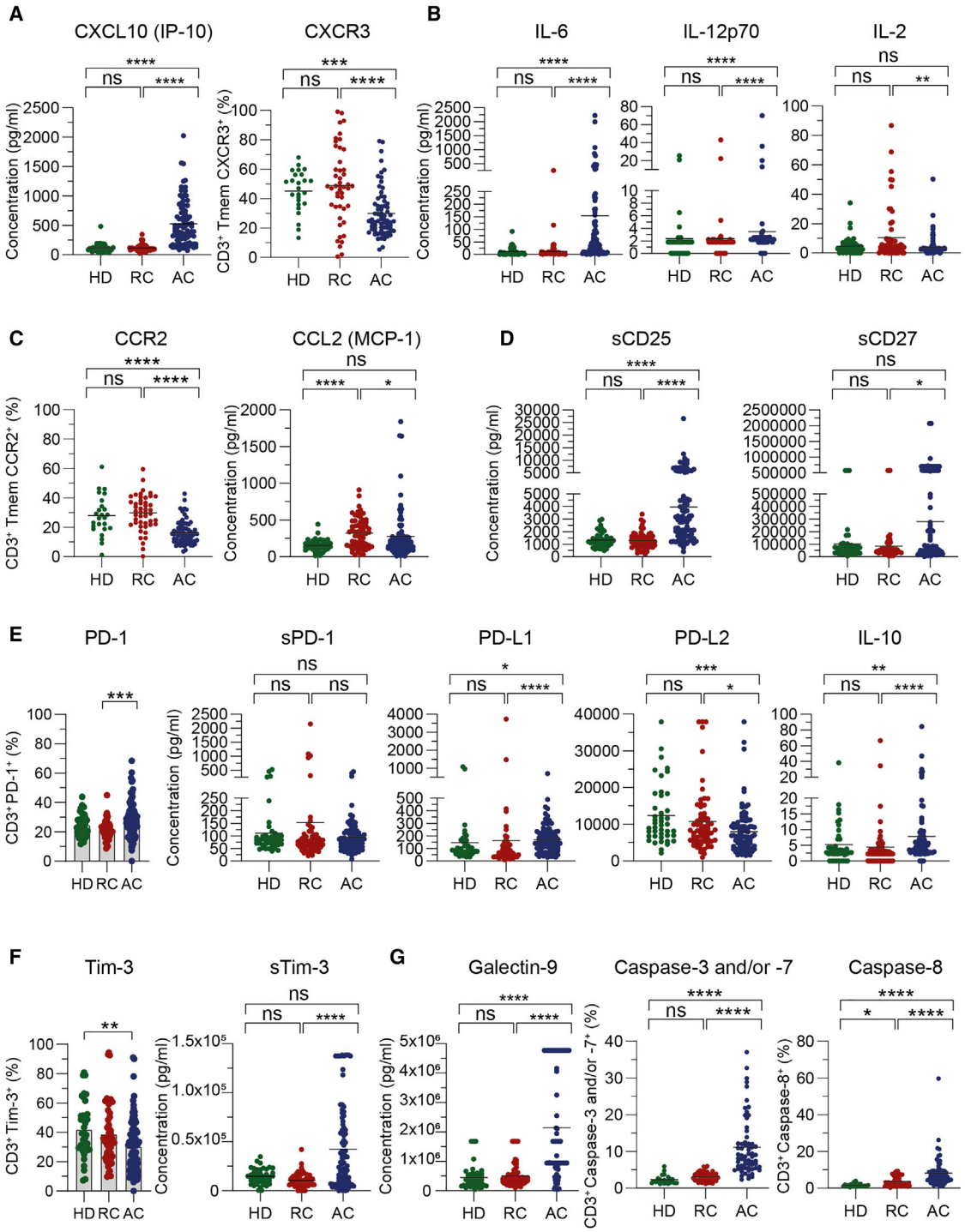

Figure 6. Overall impairment of T cell function contributes to reduced antiviral T cell immunity during COVID-19

Chemokine and immune checkpoint receptor expression on T cells as well as caspase-3 and/or -7 and caspase-8 activity in T cells were determined by flow cytometry, and plasma of healthy donors (HD, green, n = 24–43), recovered COVID-19 patients (RC, red, n = 47–66) and active COVID-19 patients (AC, blue, n = 65–92; first sample) was analyzed by LEGENDPlex assay. Statistical significance was calculated by Kruskal-Wallis test and Dunn's test for multiple comparisons: *p < 0.05, **p < 0.01, ***p < 0.001, ****p < 0.0001.

See also Figure S5.

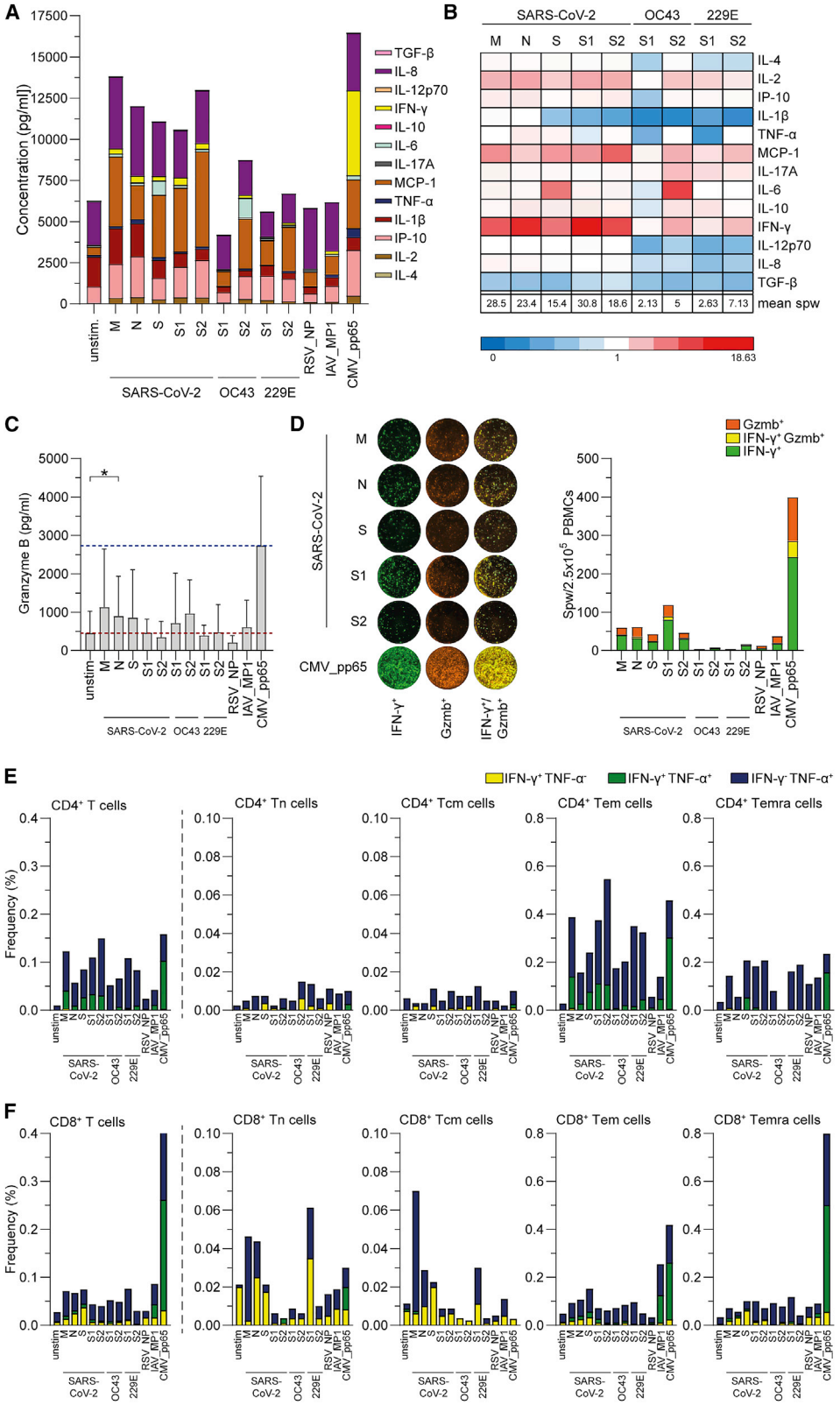

Figure 7. The signature of SARS-CoV-2-specific T cell recall responses is diverse and CD4-mediated

(A–C) Cell culture supernatants of PBMCs of recovered COVID-19 patients (RCs) stimulated with the specified peptide pools for 20 h were analyzed by (A and B) LEGENDPlex assay (n = 8; CMV_pp65: seropositive subjects only [n = 6]) or (C) ELISA (n = 7; CMV_pp65: seropositive subjects only [n = 5]). Error bars indicate standard deviation.

(legend continued on next page)

comparable between the three cohorts (Figure 6E). Compared to RCs and HDs, ACs had increased plasma programmed death ligand 1 (PD-L1) and decreased PD-L2 concentrations, independent of disease severity (Figure 6E; Figure S5E). Consistent with this high PD-L1 and PD-1 expression, ACs also had increased plasma IL-10 concentrations compared to RCs and HDs. In contrast to PD-1, the frequency of Tim-3$^+$ T cells was reduced in ACs (mean 30.18%) compared to HDs (mean 41.80%) and RCs (mean 38.59%) (Figure 6F). Likewise, soluble Tim-3 (sTim-3) in ACs was higher than in RCs and HDs and was positively correlated with disease severity (Figure 6F; Figure S5F). In addition to increased PD-1 and PD-L1 expression, ACs also had significantly higher amounts of the Tim-3 ligand galectin-9 and, consequently, higher fractions of potentially apoptotic T cells, as indicated by frequencies of cells with active caspase-3 and/or -7 and caspase-8 (mean 11.13% and 8.26%), compared to HDs (mean 2.31% and 1.76%) and RCs (mean 3.09% and 3.63%), respectively (Figure 6G). Similar to PD-L1 and PD-L2, the amount of galectin-9 and frequencies of cells with active effector caspases did not correlate with disease severity (Figure S5G).

The stimulating potential of the highly immunodominant peptide pools was further affirmed by IFN-γ and Gzmb FluoroSpot assay (Figure 7D). Despite appreciable frequencies of IFN-γ and Gzmb single-producing cells, the fraction of IFN-γ and Gzmb double-producing cells was comparably low for all tested antigens, indicating the engagement of different T cell subsets. To identify the main involved T cell populations, intracellular IFN-γ and TNF-α expression was measured after antigenic stimulation in PBMCs from RCs (Figures 7E and 7F). Among CD4$^+$ T cells, high frequencies of IFN-γ^+ TNF-α^+ double- and TNF-α^+ single-positive cells were detected in response to SARS-CoV-2_M-, N-, and S-derived peptide pools (Figure 7E). The highest frequencies were observed within CD4$^+$ Tem cells and in response to the SARS-CoV-2_S2 peptide pool. HuCoV-derived peptide pools induced mainly TNF-α. CD8$^+$ T cell responses to SARS-CoV-2 and common cold peptide pools were considerably lower than those to CMV_pp65 (CMV-seropositive donors only) (Figure 7F). In summary, these findings show that the SARS-CoV-2 immune response mainly exerts a Th1 and Th2 signature and that CD4$^+$ Tem cells produce the most cytokines in response to SARS-CoV-2 antigens.

The signature of SARS-CoV-2-specific T cell recall responses is diverse and CD4-mediated

Since T cell immunity appears to be maintained after the resolution of COVID-19, we analyzed the SARS-CoV-2-specific inflammatory signature in more detail. *In vitro* peptide pool-stimulated PBMCs from selected RCs were tested for cytokine and chemokine release and evaluated by ELISPOT assay to determine antiviral T cell frequencies (Figures 7A and 7B). SARS-CoV-2_M-, N-, and S-derived peptide pools induced high secretion of essential immune mediators, with concentrations close to those reached in response to CMV_pp65 in CMV-seropositive donors (Figure 7A). Upregulation of T helper 1 (Th1) and Th2 cytokines IL-2, IL-4, IL-10, and tumor necrosis factor-α (TNF-α) as well as of pro-inflammatory chemokines IP-10, MCP-1, and IL-8 occurred after stimulation with SARS-CoV-2_M, N, S, S1, and S2, which was higher than that obtained after stimulation with S-derived peptide pools from OC43 and 229E strains. This finding might be connected to the lower T cell frequencies against these antigens compared to SARS-CoV-2 (Figure 7B). As expected, none of the antigens resulted in an increase in transforming growth factor-β (TGF-β) secretion. The highest degree of upregulation was observed for IFN-γ, which was comparable for all peptide pools. Granzyme B (Gzmb) concentrations in the same culture supernatants were measured by ELISA (Figure 7C). None of the antigens induced Gzmb concentrations as high as those found in CMV-seropositive subjects stimulated with CMV_pp65. However, marked increases in Gzmb were observed after stimulation with SARS-CoV-2_M, N, and S as well as after stimulation with OC43_S1 and S2.

SARS-CoV-2-specific T cells for adoptive immunotherapy can be enriched from RCs

Since ACs with severe disease presented with high SARS-CoV-2-specific Abs yet low SARS-CoV-2-specific T cell frequencies, adoptive T cell transfer might be a promising treatment strategy. Therefore, an IFN-γ cytokine secretion assay (CSA) was performed to evaluate the suitability of SARS-CoV-2 overlapping peptide pools M, N, and/or S as target antigens for the generation of clinical-grade SARS-CoV-2-specific T cells (Figures S6A–S6D) (Priesner et al., 2016). The highest IFN-γ^+ T cell frequencies were detected after stimulation with all three peptide pools combined (mean 0.3%). However, the enrichment efficiency was higher for the respective peptide pools alone, while N resulted in the highest purity (mean 48.0%). In line with our finding that the majority of SARS-CoV-2-specific T cells were CD4$^+$, we observed a slightly enhanced proportion of CD4$^+$ T cells in the enriched cell fractions (data not shown). The cytotoxic potential of T cells specific for SARS-CoV-2 and CMV_pp65 was examined in CD4$^+$ and CD8$^+$ T cells sorted according to their IFN-γ production after stimulation and CSA (Figures S6E–S6G). Messenger RNA (mRNA) expression of IFN-γ was generally higher in stimulated CD4$^+$ T cells than CD8$^+$ T cells and was highest in response to S, but not as high as for CMV_pp65 (Figure S6E). Regarding GZMB and perforin (PRF1) mRNA, the highest expression was observed within positive fractions of CD8$^+$ T cells after stimulation with N (Figures S6F and S6G).

Overall, SARS-CoV-2-specific T cells against M, N and S can be efficiently generated with acceptable purity and with CD8$^+$ T cells that are more cytotoxic than CD4$^+$ T cells.

(B) Data are shown as fold change to unstimulated controls. For key to color code, see legend (n = 8).
(C) Statistical significance was calculated by Friedman's test and Dunn's test for multiple comparisons; CMV_pp65 was excluded from the analysis. *p < 0.05.
(D) Frequencies of IFN-γ and granzyme B (Gzmb)-producing cells in response to the specified peptide pools were determined by FluoroSpot. Exemplary and summarized results for n = 5 cases are shown.
(E and F) PBMCs from RC were stimulated with the specified peptide pools for 5 h, followed by flow cytometric analysis. Graphs show frequencies of IFN-γ^+ TNF-α^- (yellow), IFN-γ^+ TNF-α^+ (green), and IFN-γ^- TNF-α^+ (blue) cells within CD4$^+$ (E) and CD8$^+$ (F) T cell subsets (n = 8; CMV_pp65: seropositive subjects only [n = 6]). See also Figure S6.

DISCUSSION

A better understanding of the humoral and cellular players involved in COVID-19 disease progression and recovery is urgently needed to guide treatment strategies, predict disease outcome, and determine whether patients develop long-lasting immunity. In this study, we determined SARS-CoV-2 IgG ratios and T cell frequencies against a variety of SARS-CoV-2 proteins in HDs, RCs, and ACs in a cross-sectional manner. The analysis was extended to antigens derived from huCoV strains 229E and OC43 and antigens from RSV, IAV, and CMV. Longitudinal analysis revealed a quantitative reduction of the humoral SARS-CoV-2-specific immune response, together with constant T cell immunity up to 102 days after symptom onset. Pre-existing antiviral T cells against huCoV had beneficial effects on the development of effective T cell immunity, although during active disease a markedly reduced antiviral T cell immunity was observed.

Humoral immunity is defined by varying titers of neutralizing Abs (Amanat et al., 2020; Ni et al., 2020; Wu et al., 2020). Recent reports that COVID-19 patients become seronegative early during convalescence (Long et al., 2020; Seow et al., 2020; Ward et al., 2020) raise the question of whether recovery from COVID-19 confers immunity to reinfection, as was shown in a rhesus macaque model (Chandrashekar et al., 2020). On the other hand, it was found that IgG and neutralizing Abs remained stable for up to four months, whereas IgA and IgM decayed rapidly (Isho et al., 2020; Iyer et al., 2020). To date, a few confirmed cases of SARS-CoV-2 reinfection have been reported, and reinfection resulted in a worse course of disease in some cases (AlFehaidi et al., 2020; Iwasaki, 2021). Although it was recently reported that the number of N-specific T cells correlates with neutralizing Ab titers in convalescent subjects (Ni et al., 2020; Swadling and Maini, 2020), our study revealed no correlation in RCs but in ACs. Moreover, individuals from both cohorts with high SARS-CoV-2_S1-specific T cell frequencies had significantly higher S1 Ab values than those with low T cell frequencies, indicating that S-specific T cell responses correlated with S-specific Ab responses (Peng et al., 2020b).

It has been assumed that a certain degree of cross-reactive coronavirus immunity might influence susceptibility to COVID-19 (Braun et al., 2020; Le Bert et al., 2020; Mateus et al., 2020). Braun and colleagues suggest that pre-existing S-reactive SARS-CoV-2 $CD4^+$ T cells might be protective (Braun et al., 2020). In line with that, SARS-CoV-2-specific T cells mainly directed against M and S were detected in a fraction of SARS-CoV-2-seronegative controls in this study. Moreover, we found evidence of a correlation between huCoV_S-specific and SARS-CoV-2_S-specific T cells in RCs and ACs, implying a possibly protective role of pre-existing, potentially cross-reactive T cells (Selin et al., 2006).

The immune cell composition has been described as a partial predictor for discriminating between mild and severe COVID-19 (Odak et al., 2020; Velavan and Meyer, 2020) and extended lymphopenia with reduced T cell numbers correlates with disease severity (Chen et al., 2020; Ni et al., 2020; Wang et al., 2020). In this study, lymphocyte counts did not correlate with disease severity in hospitalized COVID-19 patients. We found that the immune cell profile was restored in patients with moderate symptoms after a relatively short period of convalescence. Moreover, M- and S-specific T cell frequencies were higher in RCs with an intermediate DSS than in those with a low DSS, whereas subjects with a high DSS had less SARS-CoV-2-specific T cells, indicating a connection between disease severity and the establishment of T cell immunity.

ACs exhibited a highly inflammatory milieu, which might be one reason for the reduced T cell immunity. Various mechanisms contributing to T cell loss are suspected, but it is assumed that the inflammatory milieu characterized by high IL-6, IL-10 and TNF-α amounts is responsible (Diao et al., 2020; Wang et al., 2020). ACs indeed, exhibited high amounts of IL-6 and IL-10, possibly driven by IP-10-induced T cell polarization. We found that the reduced number of functional antiviral T cells detected was not solely caused by a general reduction of T cell numbers, since T cell responses to CMV_pp65 were also reduced during COVID-19 and this was independent of circulating T cell numbers in the blood. Reduced frequencies of $CXCR3^+$ and $CCR2^+$ T cells might be indicative of enhanced migration, leading to a reduction of memory T cells. On the other hand, high amounts of plasma IP-10 were detected in ACs and continuously high IP-10 concentrations result in CXCR3 internalization (Metzemaekers et al., 2018), thereby possibly reducing cell migration to the place of infection and inhibiting overshooting inflammation. Moreover, it has been shown that the CCR2 and CCR5 inhibitor cenicriviroc, also known as an HIV-1 inhibitor via blockade of the HIV-1 co-receptor CCR5, inhibits SARS-CoV-2 replication *in vitro* (Okamoto et al., 2020).

Zhang et al. recently reported that sCD25 concentrations were increased in COVID-19 patients and negatively correlated with T cell numbers (Zhang et al., 2020). We also observed a significant increase in sCD25 in plasma of ACs compared to RCs and HDs, but the increase did not correlate with blood T cell count. In addition to a general T cell loss during SARS-CoV infection, T cell priming was shown to be negatively affected by elevated plasma IL-6 and reduced DC migration (Sariol and Perlman, 2020; Yoshikawa et al., 2009; Zhao et al., 2009). PD-L2, mainly produced by activated DCs, was significantly reduced, indicating impaired T cell priming during COVID-19. In contrast, ACs exhibited high concentrations of PD-L1 and high frequencies of $PD\text{-}1^+$ T cells, suggesting T cell exhaustion or anergy, which is in line with the observed high amounts of IL-10 (Zou and Chen, 2008).

PD-1 expression can be a sign of T cell activation during acute viral infection (Ahn et al., 2018). However, the PD-L1-PD-1 axis may also lead to enhanced T cell apoptosis, further supported by a significant increase in frequencies of T cells with active caspases. In addition, there is *in vitro* evidence that caspase-8-dependent cell death may be induced by a murine coronavirus as well as SARS-CoV-2 (Li et al., 2020; Zheng et al., 2020). In contrast to PD-1, $Tim\text{-}3^+$ T cell frequencies were reduced in ACs, while we observed increased amounts of sTim-3 in plasma of ACs. sTim-3 has been reported to reduce T cell activation by reducing IL-2 production (Yasinska et al., 2019); however, we did not find any decrease in IL-2. In addition, mechanisms including cell migration (IP-10-CXCR3 axis) and inhibitory molecules (PD-L1-PD-1 axis) as well as cell death (caspases-3, -7 and -8) contributed to the overall reduction of functionality in ACs. Apparently, the plasma cytokine milieu may have the potential to discriminate between mild and severe disease, suggesting their utility as prognostic markers.

In the majority of COVID-19 cases, the adaptive immune system is trained to control the virus within one to two weeks, but a minority progress to severe disease and require ICU admission (Huang et al., 2020; Rees et al., 2020). Impaired T cell function and immunosuppression may contribute to viral persistence. On the other hand, exhaustion of T cells may also prevent immunopathology (Cornberg et al., 2013). We found that ACs have generally reduced T cell immunity, as evidenced by low frequencies of antiviral T cells and the absence of CMV_pp65-reactive T cells in some CMV-seropositive ACs. The fact that ACs also had high anti-N and -S1 IgG ratios constitutes further evidence that neutralization of SARS-CoV-2 infection occurs via S1-specific Abs covering the RBD of S protein (Zhou et al., 2020). However, Abs alone appear to be insufficient for viral clearance. Adoptive transfer of SARS-CoV-2-enriched T cells from COVID-19 convalescent donors might be a therapeutic option for patients with severe disease (Ferreras et al., 2020; Leung et al., 2020), but is restricted by the availability of HLA-matched donors with sufficient SARS-CoV-2-specific T cell frequencies. The risk of graft-versus-host disease (GvHD) due to alloreactivity and the risk of induction of cytokine storm syndrome and lung damage are major concerns (Mehta et al., 2020; Ong et al., 2020). Ferreras et al. postulated that *in vitro* depletion of Tn cells via CD45RA would result in immediately available, 'off-the-shelf' SARS-CoV-2-specific memory T cell products (Ferreras et al., 2020).

Throughout this study, one HD became infected with SARS-CoV-2 and was diagnosed with WHO 3 and DSS 8 COVID-19. The T cell repertoire analysis revealed a low frequency of SARS-CoV-2-specific T cells prior to infection and an LR for M-, N-, and S-specific T cells. The subject had decreased lymphocyte numbers, diminished overall T cell responses, and increased amounts of plasma IP-10 and IL-8 early during recovery. The impact of pre-existing SARS-CoV-2-reactive T cells in naive individuals is a subject of high interest. Prospective studies in larger cohorts are needed to determine whether their presence correlates with pathology or protection from COVID-19.

A better understanding of the role of the adaptive immune system during the course of SARS-CoV-2 infection and beyond will improve COVID-19 diagnosis and prognosis and is crucial for the successful development of vaccines and cell-based therapies. Active COVID-19 patients included in this study had high SARS-CoV-2 IgG ratios yet generally reduced antiviral T cell frequencies compared to recovered COVID-19 patients, suggesting that T cells are important for the successful clearance of infection. This study provides evidence that the generally low T cell responses observed during COVID-19 are not exclusively dependent on lymphopenia, but rather on the role of PD-1 and Tim-3 as well as caspase-mediated cell death. Our study indicates that SARS-CoV-2-specific cellular immunity may be more stable and longer lasting than humoral immunity. In addition, our findings suggest that the presence of pre-existing SARS-CoV-2-specific T cells and T cells against epitopes from endemic huCoV might be protective.

LIMITATIONS OF STUDY

Our study provides evidence for a contribution of pre-existing memory $CD4^+$ and $CD8^+$ T cells against huCoV strains 229E and OC43, but pre-existing humoral responses against these strains and further huCoV strains were not considered. Moreover, we reported one case with informative immune responses before and after SARS-CoV-2 exposure. Collecting data on pre-existing cellular and humoral immunity prior to infection and during the course of the disease is very important to elucidate the role of pre-existing immunity in more detail. The results of our study are further limited to T cell responses against the huCoV S proteins and do not take into account other structural and non-structural proteins, nor HLA diversity and the resulting peptide presentation. Finally, our study relies on detection of IFN-γ secreting T cells after short-term stimulation, wheras other effector molecules such as TNF-α or Gzmb as well as the detection of lower frequencies of antiviral T cells after prolonged restimulation may provide further insight into the importance of these effector cells for viral clearance.

STAR★METHODS

Detailed methods are provided in the online version of this paper and include the following:

- KEY RESOURCES TABLE
- RESOURCE AVAILABILITY
  - Lead contact
  - Materials availability
  - Data and code availability
- EXPERIMENTAL MODEL AND SUBJECT DETAILS
  - Study population
  - Clinical definition of cohort
- METHOD DETAILS
  - Serological testing by ELISA and western blot
  - Cellular immune profiling by flow cytometry
  - Detection of antiviral T cells by IFN-γ ELISPOT
  - Detection of IFN-γ and granzyme B by FluoroSpot
  - IFN-γ CSA for enrichment of antiviral T cells
  - Intracellular cytokine staining
  - Cytokine profiling in cell culture supernatants
  - Cytokine and chemokine profiling by LEGENDPlex
  - Chemokine receptor expression on T cells
  - Caspase-3 and/or -7 and -8 activity in T cells
  - RT-PCR analysis of SARS-CoV-2-specific T cells
- QUANTIFICATION AND STATISTICAL ANALYSIS

SUPPLEMENTAL INFORMATION

Supplemental Information can be found online at https://doi.org/10.1016/j.immuni.2021.01.008.

ACKNOWLEDGMENTS

This research was funded in part by grants from the state of Lower Saxony (14 - 76103-184 CORONA-12/20), the Federal Ministry of Health (ZMVI1-2520COR804), and the German Research Foundation (DFG; Research Unit 2830 and SFB 900/B11 project ID 158989968). We are grateful to all study participants for providing samples and to the MVZ Laboratory Limbach Hannover GbR for RT-PCR analysis. Furthermore, we would like to thank Dörthe Rokitta, Nicole Neumann, Sarina Lukis, Elvira Schulde, Milena Stietzel, Juliane Ebersold, Sophie Meyer, Bach Uy Vu, Leona Schmaltz, and Marion Hitzigrath for technical support, as well as the team at the Cell Sorting Core Facility of

Hannover Medical School, which was supported in part by the Braukmann-Wittenberg Heart Foundation and the DFG.

AUTHOR CONTRIBUTIONS

Conceptualization: A.B., B.M.K., G.M.N.B., M.C., O.W., R.B., and B.E.V. Methodology: A.B., S.T., D.G., A.V., A.C.D., M.V.S., and B.E.V. Validation: A.B., S.T., A.V., A.C.D., A.R.M.K., J.M., M.V.S., and G.M.N.B. Formal analysis: A.B., S.T., D.G., A.V., A.C.D., N.G., and M.V.S. Investigation: A.B., S.T., A.V., A.C.D., D.G., N.G., C.L., M.B., I.P., M.V.S., and S.D. Resources: U.K., M.Y., M.M.H., Y.L., T.W., J.M., G.M.N.B., M.C., S.D., J.J.S., M.B., C.L., O.W., R.B., and B.E.V. Writing the original draft: A.B., S.T., and B.E.V. Visualization: A.B. and S.T. Supervision: B.E.V. Project administration: B.E.V. Grant acquisition: R.B. and B.E.V.

DECLARATION OF INTERESTS

The authors declare that they have no competing interests. The funders played no role in designing the study, in collecting, analyzing, or interpreting the data, in writing the manuscript, or in the decision to publish the results.

Received: July 20, 2020
Revised: November 12, 2020
Accepted: January 13, 2021
Published: February 9, 2021

REFERENCES

Ahn, E., Araki, K., Hashimoto, M., Li, W., Riley, J.L., Cheung, J., Sharpe, A.H., Freeman, G.J., Irving, B.A., and Ahmed, R. (2018). Role of PD-1 during effector CD8 T cell differentiation. Proc. Natl. Acad. Sci. USA *115*, 4749–4754.

AlFehaidi, A., Ahmed, S.A., and Hamed, E. (2020). A case of SARS-CoV-2 re-infection. J. Infect. *25*, https://doi.org/10.1016/j.jinf.2020.10.019.

Amanat, F., Stadlbauer, D., Strohmeier, S., Nguyen, T.H.O., Chromikova, V., McMahon, M., Jiang, K., Arunkumar, G.A., Jurczyszak, D., Polanco, J., et al. (2020). A serological assay to detect SARS-CoV-2 seroconversion in humans. Nat. Med. *26*, 1033–1036.

Baruah, V., and Bose, S. (2020). Immunoinformatics-aided identification of T cell and B cell epitopes in the surface glycoprotein of 2019-nCoV. J. Med. Virol. *92*, 495–500.

Behrens, G.M.N., Cossmann, A., Stankov, M.V., Schulte, B., Streeck, H., Förster, R., Bosnjak, B., Willenzon, S., Boeck, A.L., Thu Tran, A., et al. (2020). Strategic Anti-SARS-CoV-2 Serology Testing in a Low Prevalence Setting: The COVID-19 Contact (CoCo) Study in Healthcare Professionals. Infect. Dis. Ther. *9*, 837–849.

Bieling, M., Tischer, S., Kalinke, U., Blasczyk, R., Buus, S., Maecker-Kolhoff, B., and Eiz-Vesper, B. (2017). Personalized adoptive immunotherapy for patients with EBV-associated tumors and complications: Evaluation of novel naturally processed and presented EBV-derived T-cell epitopes. Oncotarget *9*, 4737–4757.

Braun, J., Loyal, L., Frentsch, M., Wendisch, D., Georg, P., Kurth, F., Hippenstiel, S., Dingeldey, M., Kruse, B., Fauchere, F., et al. (2020). SARS-CoV-2-reactive T cells in healthy donors and patients with COVID-19. Nature *587*, 270–274.

Bunse, C.E., Fortmeier, V., Tischer, S., Zilian, E., Figueiredo, C., Witte, T., Blasczyk, R., Immenschuh, S., and Eiz-Vesper, B. (2015). Modulation of heme oxygenase-1 by metalloporphyrins increases anti-viral T cell responses. Clin. Exp. Immunol. *179*, 265–276.

Chandrashekar, A., Liu, J., Martinot, A.J., McMahan, K., Mercado, N.B., Peter, L., Tostanoski, L.H., Yu, J., Maliga, Z., Nekorchuk, M., et al. (2020). SARS-CoV-2 infection protects against rechallenge in rhesus macaques. Science *369*, 812–817.

Chen, X., Zhao, B., Qu, Y., Chen, Y., Xiong, J., Feng, Y., Men, D., Huang, Q., Liu, Y., Yang, B., et al. (2020). Detectable Serum Severe Acute Respiratory Syndrome Coronavirus 2 Viral Load (RNAemia) Is Closely Correlated With Drastically Elevated Interleukin 6 Level in Critically Ill Patients With Coronavirus Disease 2019. Clin. Infect. Dis. *71*, 1937–1942.

Cornberg, M., Kenney, L.L., Chen, A.T., Waggoner, S.N., Kim, S.K., Dienes, H.P., Welsh, R.M., and Selin, L.K. (2013). Clonal exhaustion as a mechanism to protect against severe immunopathology and death from an overwhelming CD8 T cell response. Front. Immunol. *4*, 475.

Diao, B., Wang, C., Tan, Y., Chen, X., Liu, Y., Ning, L., Chen, L., Li, M., Liu, Y., Wang, G., et al. (2020). Reduction and Functional Exhaustion of T Cells in Patients With Coronavirus Disease 2019 (COVID-19). Front. Immunol. *11*, 827.

Ferreras, C., Pascual-Miguel, B., Mestre-Durán, C., Navarro-Zapata, A., Clares-Villa, L., Martín-Cortázar, C., De Paz, R., Marcos, A., Vicario, J.L., Balas, A., et al. (2020). SARS-CoV-2 specific memory T lymphocytes from COVID-19 convalescent donors: identification, biobanking and large-scale production for Adoptive Cell Therapy. bioRxiv, 2020.2010.2023.352294.

Grifoni, A., Weiskopf, D., Ramirez, S.I., Mateus, J., Dan, J.M., Moderbacher, C.R., Rawlings, S.A., Sutherland, A., Premkumar, L., Jadi, R.S., et al. (2020). Targets of T Cell Responses to SARS-CoV-2 Coronavirus in Humans with COVID-19 Disease and Unexposed Individuals. Cell *181*, 1489–1501.e15.

Huang, I., and Pranata, R. (2020). Lymphopenia in severe coronavirus disease-2019 (COVID-19): systematic review and meta-analysis. J. Intensive Care *8*, 36.

Huang, C., Wang, Y., Li, X., Ren, L., Zhao, J., Hu, Y., Zhang, L., Fan, G., Xu, J., Gu, X., et al. (2020). Clinical features of patients infected with 2019 novel coronavirus in Wuhan, China. Lancet *395*, 497–506.

Isho, B., Abe, K.T., Zuo, M., Jamal, A.J., Rathod, B., Wang, J.H., Li, Z., Chao, G., Rojas, O.L., Bang, Y.M., et al. (2020). Persistence of serum and saliva antibody responses to SARS-CoV-2 spike antigens in COVID-19 patients. Sci. Immunol. *5*, https://doi.org/10.1126/sciimmunol.abe5511.

Iwasaki, A. (2021). What reinfections mean for COVID-19. Lancet Infect. Dis. *21*, 3–5.

Iyer, A.S., Jones, F.K., Nodoushani, A., Kelly, M., Becker, M., Slater, D., Mills, R., Teng, E., Kamruzzaman, M., Garcia-Beltran, W.F., et al. (2020). Persistence and decay of human antibody responses to the receptor binding domain of SARS-CoV-2 spike protein in COVID-19 patients. Sci. Immunol. *5*, https://doi.org/10.1126/sciimmunol.abe0367.

Ju, B., Zhang, Q., Ge, J., Wang, R., Sun, J., Ge, X., Yu, J., Shan, S., Zhou, B., Song, S., et al. (2020). Human neutralizing antibodies elicited by SARS-CoV-2 infection. Nature *584*, 115–119.

Kissler, S.M., Tedijanto, C., Goldstein, E., Grad, Y.H., and Lipsitch, M. (2020). Projecting the transmission dynamics of SARS-CoV-2 through the postpandemic period. Science *368*, 860–868.

Krammer, F., and Simon, V. (2020). Serology assays to manage COVID-19. Science *368*, 1060–1061.

Kuri-Cervantes, L., Pampena, M.B., Meng, W., Rosenfeld, A.M., Ittner, C.A.G., Weisman, A.R., Agyekum, R.S., Mathew, D., Baxter, A.E., Vella, L.A., et al. (2020). Comprehensive mapping of immune perturbations associated with severe COVID-19. Sci. Immunol. *5*, https://doi.org/10.1126/sciimmunol.abd7114.

Le Bert, N., Tan, A.T., Kunasegaran, K., Tham, C.Y.L., Hafezi, M., Chia, A., Chng, M.H.Y., Lin, M., Tan, N., Linster, M., et al. (2020). SARS-CoV-2-specific T cell immunity in cases of COVID-19 and SARS, and uninfected controls. Nature *584*, 457–462.

Leung, W., Soh, T.G., Linn, Y.C., Low, J.G.-H., Loh, J., Chan, M., Chng, W.J., Koh, L.P., Poon, M.L.-M., Ng, K.P., et al. (2020). SUCCESSFUL MANUFACTURING OF CLINICAL-GRADE SARS-CoV-2 SPECIFIC T CELLS FOR ADOPTIVE CELL THERAPY. medRxiv. https://doi.org/10.1101/2020.04.24.20077487.

Li, S., Zhang, Y., Guan, Z., Li, H., Ye, M., Chen, X., Shen, J., Zhou, Y., Shi, Z.L., Zhou, P., and Peng, K. (2020). SARS-CoV-2 triggers inflammatory responses and cell death through caspase-8 activation. Signal Transduct. Target. Ther. *5*, 235.

Long, Q.X., Liu, B.Z., Deng, H.J., Wu, G.C., Deng, K., Chen, Y.K., Liao, P., Qiu, J.F., Lin, Y., Cai, X.F., et al. (2020). Antibody responses to SARS-CoV-2 in patients with COVID-19. Nat. Med. *26*, 845–848.

Mateus, J., Grifoni, A., Tarke, A., Sidney, J., Ramirez, S.I., Dan, J.M., Burger, Z.C., Rawlings, S.A., Smith, D.M., Phillips, E., et al. (2020). Selective and

cross-reactive SARS-CoV-2 T cell epitopes in unexposed humans. Science *370*, 89–94.

Mathew, D., Giles, J.R., Baxter, A.E., Oldridge, D.A., Greenplate, A.R., Wu, J.E., Alanio, C., Kuri-Cervantes, L., Pampena, M.B., D'Andrea, K., et al.; UPenn COVID Processing Unit (2020). Deep immune profiling of COVID-19 patients reveals distinct immunotypes with therapeutic implications. Science *369*, https://doi.org/10.1126/science.abc8511.

Mehta, P., McAuley, D.F., Brown, M., Sanchez, E., Tattersall, R.S., and Manson, J.J.; HLH Across Speciality Collaboration, UK (2020). COVID-19: consider cytokine storm syndromes and immunosuppression. Lancet *395*, 1033–1034.

Metzemaekers, M., Vanheule, V., Janssens, R., Struyf, S., and Proost, P. (2018). Overview of the Mechanisms that May Contribute to the Non-Redundant Activities of Interferon-Inducible CXC Chemokine Receptor 3 Ligands. Front. Immunol. *8*, 1970.

Ni, L., Ye, F., Cheng, M.L., Feng, Y., Deng, Y.Q., Zhao, H., Wei, P., Ge, J., Gou, M., Li, X., et al. (2020). Detection of SARS-CoV-2-Specific Humoral and Cellular Immunity in COVID-19 Convalescent Individuals. Immunity *52*, 971–977.e3.

Odak, I., Barros-Martins, J., Bošnjak, B., Stahl, K., David, S., Wiesner, O., Busch, M., Hoeper, M.M., Pink, I., Welte, T., et al. (2020). Reappearance of effector T cells is associated with recovery from COVID-19. EBioMedicine *57*, 102885.

Okamoto, M., Toyama, M., and Baba, M. (2020). The chemokine receptor antagonist cenicriviroc inhibits the replication of SARS-CoV-2 in vitro. Antiviral Res. *182*, 104902.

Ong, E.Z., Chan, Y.F.Z., Leong, W.Y., Lee, N.M.Y., Kalimuddin, S., Haja Mohideen, S.M., Chan, K.S., Tan, A.T., Bertoletti, A., Ooi, E.E., and Low, J.G.H. (2020). A Dynamic Immune Response Shapes COVID-19 Progression. Cell Host Microbe *27*, 879–882.e2.

Peng, Y., Mentzer, A.J., Liu, G., Yao, X., Yin, Z., Dong, D., Dejnirattisai, W., Rostron, T., Supasa, P., Liu, C., et al. (2020a). Broad and strong memory CD4 $^{+}$ and CD8 $^{+}$ T cells induced by SARS-CoV-2 in UK convalescent COVID-19 patients. bioRxiv *8*, https://doi.org/10.1101/2020.06.05.134551.

Peng, Y., Mentzer, A.J., Liu, G., Yao, X., Yin, Z., Dong, D., Dejnirattisai, W., Rostron, T., Supasa, P., Liu, C., et al.; Oxford Immunology Network Covid-19 Response T cell Consortium; ISARIC4C Investigators (2020b). Broad and strong memory CD4^{+} and CD8^{+} T cells induced by SARS-CoV-2 in UK convalescent individuals following COVID-19. Nat. Immunol. *21*, 1336–1345.

Priesner, C., Esser, R., Tischer, S., Marburger, M., Aleksandrova, K., Maecker-Kolhoff, B., Heuft, H.G., Goudeva, L., Blasczyk, R., Arseniev, L., et al. (2016). Comparative Analysis of Clinical-Scale IFN-γ-Positive T-Cell Enrichment Using Partially and Fully Integrated Platforms. Front. Immunol. *7*, 393.

Rees, E.M., Nightingale, E.S., Jafari, Y., Waterlow, N.R., Clifford, S., B Pearson, C.A., Group, C.W., Jombart, T., Procter, S.R., and Knight, G.M. (2020). COVID-19 length of hospital stay: a systematic review and data synthesis. BMC Med. *18*, https://doi.org/10.1186/s12916-020-01726-3.

Rudolf-Oliveira, R.C., Gonçalves, K.T., Martignago, M.L., Mengatto, V., Gaspar, P.C., de Moraes, A.C., da Silva, R.M., Bazzo, M.L., and Santos-Silva, M.C. (2015). Determination of lymphocyte subset reference ranges in peripheral blood of healthy adults by a dual-platform flow cytometry method. Immunol. Lett. *163*, 96–101.

Sariol, A., and Perlman, S. (2020). Lessons for COVID-19 Immunity from Other Coronavirus Infections. Immunity *53*, 248–263.

Schögler, A., Stokes, A.B., Casaulta, C., Regamey, N., Edwards, M.R., Johnston, S.L., Jung, A., Moeller, A., Geiser, T., and Alves, M.P. (2016). Interferon response of the cystic fibrosis bronchial epithelium to major and minor group rhinovirus infection. J. Cyst. Fibros. *15*, 332–339.

Sekine, T. (2020). Critical Review of the Literature on Chest CT and Coronavirus Disease (COVID-19): Data Adjustment. AJR Am. J. Roentgenol. *215*, W27.

Selin, L.K., Brehm, M.A., Naumov, Y.N., Cornberg, M., Kim, S.K., Clute, S.C., and Welsh, R.M. (2006). Memory of mice and men: CD8+ T-cell cross-reactivity and heterologous immunity. Immunol. Rev. *211*, 164–181.

Seow, J., Graham, C., Merrick, B., Acors, S., Pickering, S., Steel, K.J.A., Hemmings, O., O'Byrne, A., Kouphou, N., Galao, R.P., et al. (2020). Longitudinal observation and decline of neutralizing antibody responses in the three months following SARS-CoV-2 infection in humans. Nat. Microbiol. *5*, 1598–1607.

Swadling, L., and Maini, M.K. (2020). T cells in COVID-19 - united in diversity. Nat. Immunol. *21*, 1307–1308.

Tischer, S., Dieks, D., Sukdolak, C., Bunse, C., Figueiredo, C., Immenschuh, S., Borchers, S., Stripecke, R., Maecker-Kolhoff, B., Blasczyk, R., and Eiz-Vesper, B. (2014). Evaluation of suitable target antigens and immunoassays for high-accuracy immune monitoring of cytomegalovirus and Epstein-Barr virus-specific T cells as targets of interest in immunotherapeutic approaches. J. Immunol. Methods *408*, 101–113.

Vabret, N., Britton, G.J., Gruber, C., Hegde, S., Kim, J., Kuksin, M., Levantovsky, R., Malle, L., Moreira, A., Park, M.D., et al.; Sinai Immunology Review Project (2020). Immunology of COVID-19: Current State of the Science. Immunity *52*, 910–941.

Velavan, T.P., and Meyer, C.G. (2020). Mild versus severe COVID-19: Laboratory markers. Int. J. Infect. Dis. *95*, 304–307.

Wang, D., Hu, B., Hu, C., Zhu, F., Liu, X., Zhang, J., Wang, B., Xiang, H., Cheng, Z., Xiong, Y., et al. (2020). Clinical Characteristics of 138 Hospitalized Patients With 2019 Novel Coronavirus-Infected Pneumonia in Wuhan, China. JAMA *323*, 1061–1069.

Ward, H., Cooke, G., Atchison, C., Whitaker, M., Elliott, J., Moshe, M., Brown, J.C., Flower, B., Daunt, A., Ainslie, K., et al. (2020). Declining prevalence of antibody positivity to SARS-CoV-2: a community study of 365,000 adults. medRxiv, 2020.2010.2026.20219725.

Weiskopf, D., Schmitz, K.S., Raadsen, M.P., Grifoni, A., Okba, N.M.A., Endeman, H., van den Akker, J.P.C., Molenkamp, R., Koopmans, M.P.G., van Gorp, E.C.M., et al. (2020). Phenotype and kinetics of SARS-CoV-2-specific T cells in COVID-19 patients with acute respiratory distress syndrome. Sci. Immunol. *5*, https://doi.org/10.1126/sciimmunol.abd2071.

WHO (2020). COVID-19 Therapeutic Trial Synopsis.

Wu, Y., Li, C., Xia, S., Tian, X., Kong, Y., Wang, Z., Gu, C., Zhang, R., Tu, C., Xie, Y., et al. (2020). Identification of Human Single-Domain Antibodies against SARS-CoV-2. Cell Host Microbe *27*, 891–898 e5.

Yasinska, I.M., Sakhnevych, S.S., Pavlova, L., Teo Hansen Selnø, A., Teuscher Abeleira, A.M., Benlaouer, O., Gonçalves Silva, I., Mosimann, M., Varani, L., Bardelli, M., et al. (2019). The Tim-3-Galectin-9 Pathway and Its Regulatory Mechanisms in Human Breast Cancer. Front. Immunol. *10*, 1594.

Yoshikawa, N., Yoshikawa, T., Hill, T., Huang, C., Watts, D.M., Makino, S., Milligan, G., Chan, T., Peters, C.J., and Tseng, C.T. (2009). Differential virological and immunological outcome of severe acute respiratory syndrome coronavirus infection in susceptible and resistant transgenic mice expressing human angiotensin-converting enzyme 2. J. Virol. *83*, 5451–5465.

Zhang, Y., Wang, X., Li, X., Xi, D., Mao, R., Wu, X., Cheng, S., Sun, X., Yi, C., Ling, Z., et al. (2020). Potential contribution of increased soluble IL-2R to lymphopenia in COVID-19 patients. Cell. Mol. Immunol. *17*, 878–880.

Zhao, J., Zhao, J., Van Rooijen, N., and Perlman, S. (2009). Evasion by stealth: inefficient immune activation underlies poor T cell response and severe disease in SARS-CoV-infected mice. PLoS Pathog. *5*, e1000636.

Zheng, M., Williams, E.P., Malireddi, R.K.S., Karki, R., Banoth, B., Burton, A., Webby, R., Channappanavar, R., Jonsson, C.B., and Kanneganti, T.D. (2020). Impaired NLRP3 inflammasome activation/pyroptosis leads to robust inflammatory cell death via caspase-8/RIPK3 during coronavirus infection. J. Biol. Chem. *295*, 14040–14052.

Zhou, F., Yu, T., Du, R., Fan, G., Liu, Y., Liu, Z., Xiang, J., Wang, Y., Song, B., Gu, X., et al. (2020). Clinical course and risk factors for mortality of adult inpatients with COVID-19 in Wuhan, China: a retrospective cohort study. Lancet *395*, 1054–1062.

Zou, W., and Chen, L. (2008). Inhibitory B7-family molecules in the tumour microenvironment. Nat. Rev. Immunol. *8*, 467–477.

STAR★METHODS

KEY RESOURCES TABLE

REAGENT or RESOURCE	SOURCE	IDENTIFIER
Antibodies		
APC-Cy7 anti-CD45	BD Biosciences	Cat#641417, Clone 2D1; RRID: 2800453
AlexaFluor 700 anti-CD45	BioLegend	Cat#368514, Clone 2D1; RRID: 2566374
Pacific Blue anti-CD45	BioLegend	Cat#304022, Clone HI30; RRID: 493655
FITC anti-CD3	BD Biosciences	Cat#345764, Clone SK7
PE anti-CD3ÜBackspace	BioLegend	Cat#300407, Clone UCHT1; RRID: AB_314061
APC anti-CD8	BD Biosciences	Cat#345775, Clone SK1; RRID: 2868803
PE-Cy7 anti-CD8	BioLegend	Cat#344712, Clone SK1; RRID: 2044008
PerCP anti-CD4	BD Biosciences	Cat#345770, Clone SK3; RRID: 2868798
AlexaFluor 700 anti-CD19	BD Biosciences	Cat#557921, Clone HIB19; RRID: 396942
BV510 anti-CD19	BioLegend	Cat#302242, Clone HIB19; RRID: 2568668
PE anti-CD56	BD Biosciences	Cat#345812, Clone NCAM16.2; RRID: 2629216
BV510 anti-CD14	BD Biosciences	Cat#563079, Clone MφP9; RRID: 2737993
BV605 anti-CD45RA	BioLegend	Cat#304134, Clone HI100; RRID: 2563814
BV421 anti-CD62L	BioLegend	Cat#304828, Clone DREG-56; RRID: 2562914
BV510 anti-CD62L	BioLegend	Cat#304844, Clone DREG-56; RRID: 2617003
FITC anti-CD62L	BioLegend	Cat#304804, Clone DREG-56; RRID: 314464
APC-Cy7 anti-CD20	BioLegend	Cat#302314, Clone 2H7; RRID: 314262
BV421 anti-CD27	BioLegend	Cat#356418, Clone M-T271; RRID: 2562559
APC anti-CD38	BioLegend	Cat#356606, Clone HB-7; RRID: 2561902
PerCP anti-CD24	BioLegend	Cat#311114, Clone ML5; RRID: 2561284
PE anti-IgD	BioLegend	Cat#348204, Clone IA6-2; RRID: 10553900
FITC anti-IgM	BioLegend	Cat#314506, Clone MHM-88; RRID: 493009
PE anti PD-1	BioLegend	Cat#329906, Clone EH12.2H7; RRID: 940483
AlexaFluor 700 anti-CD4	BD Biosciences	Cat#557922, Clone RPA-T4; RRID: 396943
PE anti-IFN-γ	BioLegend	Cat#502509, Clone 4S.B3; RRID: 315234
APC anti-TNF-α	BioLegend	Cat#502912, Clone Mab11; RRID: 315264
PE-Cy7 anti-TCRγ/δ	BD Biosciences	Cat#655410, Clone 11F2; RRID: 2870377
BV510 anti-CXCR3	BioLegend	Cat#353726, Clone G025H7; RRID: 2563642
BV605 anti-CCR2	BioLegend	Cat#357214, Clone K036C2; RRID: 2563876
BV421 anti-Tim-3	BioLegend	Cat#345008, Clone F38-2E2; RRID: 11218598
mAb-AP IFNγ T-Track	Lophius	Cat#123600002
Biological Samples		
Blood samples HD (peripheral blood of healthy adult donors from alloCELL registry)	Hannover Medical School	http:/allocell.org
Plasma samples HD (peripheral blood of healthy adult donors from alloCELL registry)	Hannover Medical School	http:/allocell.org
Blood samples RC (recovered COVID-19 patients)	Hannover Medical School	N/A
Plasma samples RC (recovered COVID-19 patients)	Hannover Medical School	N/A
Blood samples AC (patients with active COVID-19)	Hannover Medical School, University Hospital Essen	N/A
Plasma samples AC (patients with active COVID-19)	Hannover Medical School, University Hospital Essen	N/A
AB-Serum	CCPro	Cat#S-41-M

(*Continued on next page*)

Continued

REAGENT or RESOURCE	SOURCE	IDENTIFIER
Chemicals, Peptides, and Recombinant Proteins		
7AAD	BD Biosciences	Cat#559925; RRID: 2869266
CellEvent Caspase-3/7 Green Detection Reagent	Invitrogen	Cat#C10423
CaspGLOW Fluorescein Active Caspase-8 Staining Kit	Invitrogen	Cat#88-7005-42; RRID: 2574940
TruCount Tubes	BD Biosciences	Cat#340334
Lysing Solution	BD Biosciences	Cat#349202; RRID: 2868862
Lysing Solution	Beckman Coulter	Cat#A07799
RPMI1640	LONZA	Cat#BE12-702F
Lymphosep	CCPro	Cat#PL-15-L
PBS	LONZA	Cat#BE17-512F
WFI	Lonza	Cat#BE17-724F
TexMACS Medium	Miltenyi Biotec	Cat#170-076-307
AutoMACS Rising Solution	Miltenyi Biotec	Cat#130-091-222
BCIP/NBT	Serva	Cat#15246.01
Streptavidin-Alkaline Phosphatase	Mabtech	Cat#12360002-S
PMA	Sigma	Cat#P1585
Ionomycin	Sigma	Cat#I9657
Brefeldin A	BioLegend	Cat#420601
anti-CD3/anti-CD28 Dynabeads	Thermo Fisher Scientific	Cat#111.31D
Staphylococcus Enterotoxin B (SEB)	Sigma	Cat#S4881
CMVpp65 peptide pool	Miltenyi Biotec	Cat#130-093-435
SARS-CoV-2 M peptide pool	Miltenyi Biotec	Cat#130-126-703
SARS-CoV-2 N peptide pool	Miltenyi Biotec	Cat#130-126-699
SARS-CoV-2 S peptide pool	Miltenyi Biotec	Cat#130-126-701
SARS-CoV-2 S peptide pool vial 1 and vial 2	JPT	Cat#PM-WCPV-S
SARS-CoV-2 VEMP	JPT	Cat#PM-WCPV-VEMP
SARS-CoV-2 NS6 peptide pool	JPT	Cat#PM-WCPV-NS6
SARS-CoV-2 AP3A peptide pool	JPT	Cat#PM-WCPV-AP3A
SARS-CoV-2 NS7A peptide pool	JPT	Cat#PM-WCPV-NS7A
SARS-CoV-2 NS7B peptide pool	JPT	Cat#PM-WCPV-NS7B
SARS-CoV-2 NS8 peptide pool	JPT	Cat#PM-WCPV-NS8
SARS-CoV-2 ORF10 peptide pool	JPT	Cat#PM-WCPV-ORF10
SARS-CoV-2 ORF9B peptide pool	JPT	Cat# PM-WCPV-ORF9B
SARS-CoV-2 Y14 peptide pool	JPT	Cat#PM-WCPV-Y14
huCoV 229E	JPT	Cat#PM-229E-S-1
huCoV OC43	JPT	Cat#PM-OC43-S-1
human Respiratory Syncytial Virus RSV (HRSVA nucleoprotein, NP)	JPT	Cat#PM-HRSVB-NCPN
human Influenza virus (matrix protein 1, MP1)	JPT	Cat#PM-INFA-MP1-H1N1
Critical Commercial Assays		
recomLine CMV IgG	Mikrogen	Cat#5572
recomLine SARS-CoV2 IgG	Mikrogen	Cat#7374
anti-SARS-COV-2 S1 spike protein domain/receptor binding domain IgG ELISA	Euroimmun	Cat#EI 2606-9601 G, A
anti-SARS-COV-2 NCP IgG ELISA	Euroimmun	Cat#EI 2606-9601-2 G, M
IFN-γ Secretion Assay	Miltenyi Biotec	Cat#130-054-201
MS Column	Miltenyi Biotec	Cat#130-042-201
Ready-MTP basic IFNγ T-Track	Lophius	Cat#12100010
FluorSpot assay	Mabtech	Cat#FSP-0110-10

(*Continued on next page*)

Continued		
REAGENT or RESOURCE	SOURCE	IDENTIFIER
IntraPrep Permeabilizaton Reagent	Beckman Coulter	Cat#A07803
Human Essential Immune Response Panel LegendPlex	BioLegend	Cat#740930
HU Immune Checkpoint Panel LegendPlex	BioLegend	Cat#740866
Granzyme B ELISA	Invitrogen	Cat#BMS2027; RRID: 2575322
TaqMan Gene Expression Master Mix	Applied Biosystems	Cat#4369016
RNeasy Mini Kit	QIAGEN	Cat#74104
Deposited Data		
analyzed data	This paper	N/A
Oligonucleotides		
GAPDH TaqMan® Gene Expression Assays	Applied Biosystems	Hs_027588991_g1
IFNγ TaqMan® Gene Expression Assays	Applied Biosystems	Hs_00989291_m1
Granzyme B TaqMan® Gene Expression Assays	Applied Biosystems	Hs_01554355_m1
Perforin TaqMan® Gene Expression Assays	Applied Biosystems	Hs_00169473_m1
Software and Algorithms		
BD FACSDiva Software version 8.0.1	BD Biosciences	N/A
FlowJo™ v10.6.2	FlowJoTM LLC, BD Biosciences	https://www.flowjo.com
Prism Version 8.2.0	GraphPad Software	https://www.graphpad.com

RESOURCE AVAILABILITY

Lead contact

Further information and requests for resources and reagents should be direct to and will be fulfilled by the Lead Contact, Britta Eiz-Vesper (eiz-vesper.britta@mh-hannover.de).

Materials availability

This study did not generate new unique reagents.

Data and code availability

The published article includes all datasets generated or analyzed during this study. This study did not generate codes.

EXPERIMENTAL MODEL AND SUBJECT DETAILS

Study population

The study was approved by the Internal Review Board of Hannover Medical School (MHH, approval number 3639_2017, 9001_BO-K, 9255_BO_K_2020), and all patients and donors were recruited from MHH. Following written informed consent, peripheral blood samples from 82 adult healthy donors (HDs) from the alloCELL registry (controls), 204 recovered COVID-19 patients (RCs) and 92 patients with active COVID-19 (ACs) were tested between April and October 2020. PBMCs were isolated from either whole blood samples (RCs and ACs) or from residual blood samples from platelet and plasma apheresis disposables used for routine collection (RCs and controls). SARS-CoV-2-negative samples collected from healthy adult donors in 2020 were used for the analysis. Age and sex of all patients and donors are displayed in Figure 1. Samples from RCs and ACs were collected 29-175 days and 0-49 days from the time of the first positive SARS-CoV-2 reverse transcriptase polymerase chain reaction (RT-PCR) test or start of their symptoms, respectively. Up to five follow-up samples from ACs were obtained within five weeks of first sampling. Follow-up samples from RCs were obtained between 5 and 154 days after first sampling.

Clinical definition of cohort

All recovered and active COVID-19 cases were confirmed by SARS-CoV-2 RT-PCR testing of upper respiratory tract (nose or throat) swabs in accredited laboratories using Real-Time-PCR-Tests SARS-CoV-2 RUO (R-biopharm), Allplex 2019-nCOV Assay (Seegene), RealStar SARS-CoV-2 RT-PCR Kit (Altona Diagnostics), Xpert Xpress SARS-CoV-2 (Cepheid) or Abbott RealTime SARS-CoV-2 assay (Abbott). According to WHO recommendations, severity was graded as "uninfected" (score 0), "ambulatory" (score 1-2), "hospitalized, mild or severe disease" (score 3-7), or "death" (score 8). RCs were additionally scored based on the following symptoms: flu-like symptoms (dizziness, headache, chills, runny nose; 1 point), gastrointestinal complaints (diarrhea, vomiting, excessive; 1 point), fever (3 points), cough and respiratory problems (sore throat, lung pain, shortness of breath; 2 points) neurological symptoms

(impaired sense of taste or smell; 3 points), hospitalization (5 points), and hospitalization with ventilation (5 points); the score range was 0-20.

METHOD DETAILS

Serological testing by ELISA and western blot

All patients and donors were pretested for CMV as described previously using commercially available IgG ELISA and IgG western blot kits (recomLine CMV IgG, Mikrogen, Neuried, Germany) (Tischer et al., 2014). SARS-CoV-2 serology was performed by ELISA (anti-SARS-COV-2 S1 spike protein domain IgG and anti-SARS-COV-2 NCP, referred to as N; IgG; Euroimmun, Lübeck, Germany) according to the manufacturer's instructions. Antibody amounts are expressed as IgG ratio (optical density divided by calibrator); values below 0.8 were defined as negative, those between 0.8 and 1.1 were classified as intermediate, and values above 1.1 were defined as positive. Western blot tests (recomLine SARS-CoV2 IgG, Mikrogen, Neuried, Germany) were performed in selected individuals from all three cohorts to detect IgG directed against N protein of huCoV strains and against N, RBD and S1 proteins of SARS-CoV-2.

Cellular immune profiling by flow cytometry

All flow cytometric analyses were performed using the FACSCanto 10c cytometer (BD Biosciences, Heidelberg, Germany) and BD FACSDiva Software version 8.0.1. Cellular immune status (Panel 1), T cell activation and exhaustion (Panel 2) and B cell phenotype (Panel 3) were determined using specific markers for innate leukocytes, T cells and B cells. Briefly, cell frequencies and total cell numbers in whole blood samples were analyzed on a single-cell platform using TruCount^{TM} tubes (BD Biosciences). Cells were stained for 30 min at room temperature using anti-CD45 allophycocyanin-H7 (APC-H7) or AlexaFluor 700 (AF-700), anti-CD3 fluorescein isothiocyanate (FITC), anti-CD8 allophycocyanin (APC), anti-CD4 peridinin chlorophyll protein complex (PerCP), anti-CD19 AF-700 or Brilliant Violet (BV510), anti-CD56 phycoerythrin (PE), anti-CD14 Brilliant Violet (BV510), anti-CD45RA BV605 and anti-CD62L BV421 or BV510, anti-CD20 APC-cyanine 7 (APC-Cy7), anti-CD27 BV421, anti-CD38 APC, anti-CD24 PerCP, anti-IgD PE, anti-IgM FITC and anti-PD-1 PE monoclonal antibodies (BioLegend and BD Biosciences) either before (Panels 1 and 2) or after (Panel 3) lysis of erythrocytes using 1x Lysing Solution according to the manufacturer's instructions (Panels 1 and 2: BD Biosciences, Panel 3: Beckman Coulter, Brea, CA, USA).

Detection of antiviral T cells by IFN-γ ELISPOT

SARS-CoV-2-specific T lymphocytes were detected by IFN-γ ELISPOT assay as previously described (Bieling et al., 2017). Briefly, PBMCs were isolated from blood samples by discontinuous density gradient centrifugation, resuspended in culture medium (CM) consisting of RPMI-1640 (Lonza, Vervies, Belgium) supplemented with 10% human AB serum (C.C.pro, Oberdorla, Germany) at a concentration of $1x10^7$ cells/mL, seeded in 24-well plates and rested overnight. Rested PBMCs were co-cultured in anti-IFN-γ pre-coated ELISPOT plates (Lophius Biosciences, Regensburg, Germany) for 16-18 h at a density of $2.5x10^5$ cells/well with specific antigens of interest. Overlapping peptide pools against SARS-CoV-2 M, N and S proteins (Miltenyi Biotec, Bergisch Gladbach, Germany) were used to stimulate each sample; they were extended to the following SARS-CoV-2 proteins if PBMC counts allowed: S1 and S2, envelope small membrane protein VEMP, accessory protein 3A (AP3A), nonstructural proteins NS6, NS7A, NS7B and NS8, open reading frame proteins ORF10 and ORF9B, and Y14 (JPT, Berlin, Germany). The S peptide pool covered mainly the C-terminal domain of SARS-CoV-2 S protein supplemented with selected N-terminal epitopes, whereas S1 and S2 together covered the whole protein sequence. Pools were used at a final concentration of 1 μg of each peptide/mL peptide pool. Antigens of the S1 and S2 epitopes of huCoV strains 229E and OC43, antigens derived from human RSV (nucleoprotein, NP), IAV (matrix protein 1, MP1) (all supplied by JPT), and CMV phosphoprotein 65 (pp65; Miltenyi Biotec) were also analyzed.

Cells stimulated with staphylococcal enterotoxin B (1 μg/mL, SEB, Merck, Taufkirchen, Germany) served as positive controls, and PBMCs incubated in media alone as negative controls (NC). IFN-γ secretion was detected using streptavidin-alkaline phosphatase (Mabtech Stockholm, Sweden) and revealed by 5-13 bromo-4-chloro-3-indolyl phosphate and nitroblue tetrazolium (BCIP/NBT Liquid Substrate, Merck, Darmstadt, Germany). Spots were counted using AID ELISPOT 8.0 on an AID iSpot spectrum reader system (both from AID, Strassberg, Germany). Means of duplicate well readings were calculated and expressed as the number of spots per well (spw). The positive test threshold was set at $\geq$ 3 spw or > 2xNC + 1. Donors were divided into four groups based on spw values as follows: high responders (HR): $\geq$ 50 spw or 47 spw + 2xNC), intermediate responders (IR): $\geq$ 10 spw or 7 spw + 2xNC), low responders (LR): $\geq$ 3 spw or 2xNC), and non-responders (NR): < 3 spw or 2xNC. PBMCs were stained with anti-CD45 APC-H7, anti-CD3 FITC, anti-CD4 PerCP and anti-CD8 APC (BioLegend and BD Biosciences) for calculation of spots/10,000 $CD3^+$ T cells.

Detection of IFN-γ and granzyme B by FluoroSpot

SARS-CoV-2-specific T cell function was determined by IFN-γ and Gzmb effector molecule detection by FluoroSpot assay (Mabtech). Briefly, PBMCs were seeded into pre-coated FluoroSpot plates in CM at a density of $2.5x10^5$ cells/well and stimulated with indicated peptide pools for a period of 45 h. Negative and positive controls were carried out as described for IFN-γ ELISPOT assay. Following detection according to the manufacturer's instruction, spots were identified using the filter for FITC to identify IFN-γ-producing cells and using the filter for Cy3 to identify Gzmb-producing cells. Results were expressed as the number of spots per well (spw).

IFN-γ CSA for enrichment of antiviral T cells

The IFN-γ CSA (Miltenyi Biotec) was performed as previously described (Tischer et al., 2014). After overnight resting in TexMACS™ Medium (Miltenyi Biotec), 1x10^7 isolated PBMCs were stimulated with peptide pools of SARS-CoV-2 M, N and/or S protein (Miltenyi Biotec) alone or in combination at a final concentration of 1 μg of each peptide/mL peptide pool. Unstimulated PBMCs served as negative controls. Activated IFN-γ-secreting T cells were specifically captured during the magnetic cell sorting enrichment process using anti-IFN-γ PE antibodies and paramagnetic anti-PE microbeads. Aliquots of the respective cell fractions collected before and after enrichment were used for analysis of IFN-γ$^+$ T cell subsets by multicolor flow cytometry. The distribution of viable and dead cells in these fractions was analyzed by 7-amino-actinomycin D (7-AAD) staining (BD Biosciences). The percentage of viable IFN-γ$^+$ cells was determined by staining the cells with anti-CD45 APC-H7, anti-CD3 FITC, anti-CD8 APC and anti-CD4 AF-700 mAbs (all from BD Biosciences). At least 10,000 events were acquired in the viable CD45$^+$ leukocyte gate in each test (system: FACSCanto10c, BD Biosciences). CD3$^+$ IFN-γ$^+$ CD8$^+$ IFN-γ$^+$ and CD4$^+$ IFN-γ$^+$ T cell populations were gated based on the scatter properties of viable 7AAD$^-$ CD45$^+$ CD3$^+$ T cells.

Intracellular cytokine staining

After overnight resting, 1x10^6 isolated PBMCs were stimulated with peptide pools derived from SARS-CoV-2 M, N, S, S1 and S2 proteins (Miltenyi Biotec and JPT) at a final concentration of 1 μg of each peptide per ml peptide pool. Unstimulated PBMCs served as negative controls, and cells stimulated with phorbol 12-myristate 13-acetate (PMA; 10 ng/mL) and ionomycin (500 ng/mL, Sigma Aldrich) served as positive controls. Antigens from epitopes of huCoV strains OC43 and 229E as well as RSV_NP, IAV_MP1 (all JPT) and CMV_pp65 (Miltenyi Biotec) were also analyzed. After 1 h of incubation, 5 μg/mL Brefeldin A was added to each well (BioLegend). Following a total stimulation time of 5 h, cells were harvested and extracellularly stained with anti-CD45 Pacific Blue, anti-CD4 PerCP, anti-CD8 PE-Cy7, anti-CD45RA BV605 and anti-CD62L FITC. Subsequently, cells were fixed and permeabilized using the IntraPrep Kit according to the manufacturer's instructions (Beckman Coulter). Cells were intracellularly stained with anti-IFN-γ PE and anti-TNF-α APC. Samples were acquired on a FACSCanto 10c system (BD Biosciences), and at least 50,000 events in the CD45$^+$ lymphocyte gate were analyzed in each test.

Cytokine profiling in cell culture supernatants

After overnight resting, 1x10^6 PBMCs isolated from RCs were stimulated with peptide pools derived from SARS-CoV-2 M, N, S, S1 and S2 proteins (Miltenyi Biotec. and JPT) at a final concentration of 1 μg/mL. Unstimulated PBMCs served as negative controls, and cells stimulated with anti-CD3/anti-CD28 Dynabeads (Thermo Fisher Scientific) served as positive controls. S1 and S2 antigens of huCoV strains 229E and OC43 as well as RSV_NP, IAV_MP1 and CMV_pp65 antigens were also analyzed. After 20 h of stimulation, cell culture supernatants were collected and stored at -20°C until further processing. Cytokine and chemokine secretion was determined using the Human Essential Immune Response Panel (BioLegend).

Cytokine and chemokine profiling by LEGENDPlex

Plasma samples and antigen-stimulated cell culture supernatants were collected from all three cohorts as described above and analyzed by LEGENDPlex™ using the Human Essential Immune Response Panel and the HU Immune Checkpoint Panel 1 (BioLegend). Gzmb concentrations in cell culture supernatants were determined by ELISA according to the manufacturer's instructions (Invitrogen, Carlsbad, CA, USA).

Chemokine receptor expression on T cells

PBMCs from all three cohorts were stained with anti-CD45 APC-H7 and anti-CD3 FITC (BD Biosciences) at room temperature and washed once, followed by staining with anti-CCR2 BV605 and anti-CXCR3 BV510 (both Biolegend) at 37°C for 30 min. After final washing, samples were acquired on a FACSCanto 10c system (BD Biosciences), and at least 50,000 events in the CD45$^+$ lymphocyte gate were analyzed in each test.

Caspase-3 and/or -7 and -8 activity in T cells

PBMCs from each cohort were stained with anti-CD3 PE (BioLegend) at room temperature and washed once, followed by staining with CellEvent™ Caspase-3/7 Green Detection Reagent or eBioscience CaspGLOW™ Fluorescein Active Caspase-8 Kit (both Invitrogen) according to the manufacturer's instructions. Finally, cells were washed and dead cells stained with 7-AAD. Subsequently, samples were acquired on a FACSCanto 10c system (BD Biosciences), and at least 50,000 events in the CD45$^+$ lymphocyte gate were analyzed in each test.

RT-PCR analysis of SARS-CoV-2-specific T cells

Messenger RNA amounts of IFN-γ (IFNG), perforin (PRF1) and granzyme B (GZMB) were analyzed as previously described (Bunse et al., 2015). Briefly, total cellular RNA (RNeasy Mini Kit; QIAGEN, Hilden, Germany) was isolated from CD4$^+$ IFN-γ$^+$ and CD8$^+$ IFN-γ$^+$ T cells and their IFN-γ-negative counterparts after stimulation with overlapping peptide pools covering the M, N and S protein of SARS-CoV-2 or CMV_pp65, using 1 μg of each peptide per ml peptide pool. Subsequent cytokine detection (Cytokine Detection Kit, Miltenyi Biotec) and FACS sorting was performed using anti-CD3 FITC, anti-CD8 APC and anti-CD4 APC-Cy7 (BD Biosciences and BioLegend). The cDNA was amplified using the High Capacity cDNA Reverse Transcription Kit (Applied Biosystems, Darmstadt,

Germany). Messenger RNA amounts were quantified using inventoried mixes and TaqMan Gene Expression Master Mix (both from Applied Biosystems). Constitutively expressed glyceraldehyde 3-phosphate dehydrogenase (GAPDH) served as the reference gene. All tests were performed in duplicate, and all samples from each donor were measured on a single plate to reduce inter-assay variability.

QUANTIFICATION AND STATISTICAL ANALYSIS

Data were analyzed using Microsoft Excel 2010 (Microsoft Corporation, Redmond), FlowJo™ v10 (FlowJo™ LLC, BD Biosciences) and BD FACSDiva v8.0.1 (BD Biosciences). Graphs for statistical analysis were generated using Prism Version 8.2.0 (GraphPad Software, San Diego, California, USA). Statistical analysis was performed using a linear regression model and the Kruskal-Wallis or Friedman test followed by multiple comparison correction. Significant differences were calculated and expressed as p values (*$p < 0.05$, **$p < 0.01$, ***$p < 0.001$, ****$p < 0.0001$). Statistical details of all experiments are described in each figure legend.